SUPPORTING INFORMATION

Straightforward access to mono- and bis-cycloplatinated helicenes that display circularly polarized phosphorescence using crystallization resolution methods

Chengshuo Shen,[a] Emmanuel Anger,[a] Monika Srebro,[b] Nicolas Vanthuyne,[c] Kirandeep K. Deol,[d] Truman D. Jefferson Jr.,[d] Gilles Muller,[d] J. A. Gareth Williams,[e] Loïc Toupet,[a] Christian Roussel,[c] Jochen Autschbach,[f] RégisRéau,[a] and Jeanne Crassous[a]

General

All experiments were performed under an atmosphere of dry argon using standard Schlenk techniques. Commercially available reagents were used as received without further purification. Solvents were freshly distilled under argon from sodium/benzophenone (tetrahydrofuran, diethyl ether) or from phosphorus pentoxide (pentane, dichloromethane). Preparative separations were performed by gravity column chromatography on basic alumina (Aldrich, Type 5016A, 150 mesh, 58 Å) or silica gel (Merck Geduran 60, 0.063-0.200 mm) in 3.5-20 cm columns. ^{1}H, ^{13}C, and ^{31}P NMR spectra were recorded on Bruker Ascend 400. The ^{1}H NMR spectra show characteristic platinum satellites (^{195}Pt, I = ½, 33.8 % natural abundance), $^{3}J_{\text{Pt-H}}$ constants are observed. ^{195}Pt, ^{1}H and ^{13}C NMR chemical shifts were reported in parts per million (ppm) relative to Na_2PtCl_4 or Me_4Si as respective external standard. Assignment of proton atoms is based on COSY experiment. Assignment of carbon atoms is based on HMBC, HMQC and DEPT-135 experiments. Elemental analyses were performed by the CRMPO, University of Rennes 1. CD Specific rotations (in deg cm^2 g^{-1}) were measured in a 1 dm thermostated quartz cell on a Jasco-P1010 polarimeter. Circular dichroism (in M^{-1} cm^{-1}) was measured on a Jasco J-815 Circular Dichroism Spectrometer (IFR140 facility - Université de Rennes 1). 2-(4′-Methoxy[6]helicen-1′-yl)pyridine (±)-**1a**, [1] 1,8-bis-(2-pyridyl)-naphthalene **1b**, [2] and *R*-bis(methyl-(*p*-tolyl)sulfoxide-*S*)platinum(II)-bis-chloride [3] were prepared according to previously described procedure.

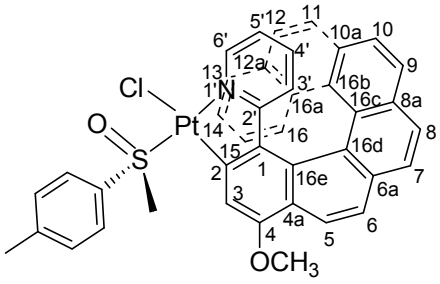

(M,R_S)-**2a**^{1}

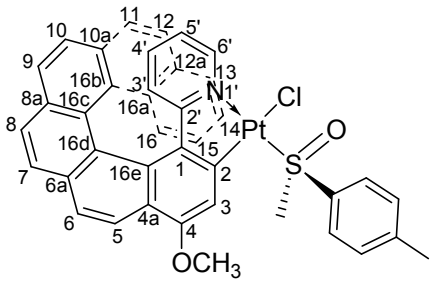

(P,R_S)-**2a**^{2}

Diastereomeric complexes (M,R_S)-2a^1 and (P,R_S)-2a^2. A mixture of 2-(4′-methoxy[6]helicen-1′-yl)pyridine (±)-**1a** (527 mg 1.21 mmol), *R*-bis(methyl-(*p*-tolyl)sulfoxide-*S*)platinum(II) chloride (1040 mg 1.81 mmol) and Na_2CO_3 (194 mg 1.83 mmol) in 10 mL toluene was refluxed under argon overnight, and concentrated in vacuum. Diastereomeric separation over a column chromatography (silica gel, heptane/ethyl acetate 3:1) was then carefully conducted (very long column > 50 cm with a diameter Φ = 5 cm). The first eluted compound (RF=0.65) afforded pure diastereomer (P,R_S)-**2a**^{2} (330 mg, 33%) as a yellow powder, while the second eluted one (RF=0.62) afforded pure diastereomer (M,R_S)-**2a**^{1} (166 mg, 18%) as orange crystals after recrystallization from the eluent mixture.

(M,R_S)-2a^1 diastereomer. ^{1}H NMR (500 MHz, C*D*Cl$_3$), δ 8.89 (AB<u>M</u>Xsystem, ^{195}Pt satellites: $^3J_{Pt\text{-}H}$ = 34 Hz, 1H, $H^{6'}$), 8.29 (d, J = 8.6 Hz, 1H, H^5), 8.11 (d, J = 8.4 Hz, 2H, H^{ortho}),8.06 (dd, J = 8.0 Hz, J = 0.9 Hz, 1H, H^{13}), 7.99 (<u>A</u>B system, J = 8.2 Hz, 1H, H^8), 7.97 (A<u>B</u> system, J = 8.2 Hz, 1H, H^7), 7.86 (d, J = 8.6 Hz, 1H, H^6), 7.86 (d, J = 8.1 Hz, 1H, H^9), 7.70 (d, J = 8.5 Hz, 1H, H^{12}), 7.61 (d, J = 8.1 Hz, 1H, H^{10}), 7.41 (ddd, J = 8.0 Hz, J = 6.9 Hz, J = 1.1 Hz, 1H, H^{14}),7.33 (d, J = 8.5 Hz, 1H, H^{11}),7.31 (d, J = 8.4 Hz, 2H, H^{meta}),7.20 (d, J = 8.5 Hz, 1H, H^{16}), 7.17 (s, ^{195}Pt satellites: $^3J_{Pt\text{-}H}$ = 52 Hz,1H, H^3), 6.71 (ddd, J = 8.5 Hz, J = 6.9 Hz, J = 1.3 Hz, 1H, H^{15}), 6.53 (<u>A</u>BMX system, 1H, $H^{5'}$), 6.51 (A<u>B</u>MX system, 1H, $H^{4'}$), 5.53 (ABM<u>X</u> system, 1H, $H^{3'}$), 3.90 (s, 3H, −OCH_3), 3.81 (s, 3H, −SOCH_3), 2.39 (s, 3H, ArCH_3).^{13}C{^{1}H} NMR (100 MHz, C*D*Cl$_3$), δ = 166.9 ($C^{2'}$), 155.8 (C^4), 147.7 ($C^{6'}$), 146.4 (C^2), 143.3 (C^{para}), 141.9 (C^{ipso}), 136.1 ($C^{4'}$), 134.5 (C^1), 132.3 (C^{12a}),132.2 (C^{8a}), 131.7 (C^{6a}), 131.3 (C^{10a}), 129.9 (C^{meta}), 128.7 (C^{16a}), 128.5 (C^{13}), 128.4 (C^{12}), 128.1 (C^{16b}), 127.5 (C^8), 127.1 (C^{16e} and C^{16c}), 127.0 (C^7), 126.5 (C^{10}),126.1 (C^9), 125.97 (C^{ortho}), 126.0 (C^{14}),125.9 (C^{16}), 125.2 (C^{11}), 125.0 (C^{15}),124.1 (C^6), 123.3 (C^{16d}), 122.7 (C^{4a}), 121.6 (C^5),118.1 ($C^{5'}$), 118.0 ($C^{3'}$), 112.2 (C^3), 56.1 (−OCH$_3$), 49.3 (−SOCH$_3$), 21.5 (ArCH$_3$). $[\alpha]_D^{23}$ = -2435, $[\phi]_D^{23}$ = -19920 (CH_2Cl_2, 10^{-4} mol·L^{-1}). Elemental analysis, calcd. (%) for $C_{40}H_{30}ClNO_2PtS$: C 58.64, H 3.69; found : C 58.50, H 3.73.

(P,R_S)-2a^2 diastereomer. ^{1}H NMR (500 MHz, C*D*Cl$_3$), δ 8.90 (ddd, J = 5.8 Hz, J = 1.8 Hz, J = 0.6 Hz, ^{195}Pt satellites: $^3J_{Pt\text{-}H}$ = 34 Hz, 1H, $H^{6'}$), 8.32 (d, J = 8.6 Hz, 1H, H^5), 8.21 (d, J = 8.5 Hz, 2H, H^{ortho}), 7.97 (<u>A</u>B system, J = 8.2 Hz, 1H, H^8), 7.96 (A<u>B</u> system, J = 8.2 Hz, 1H, H^7), 7.86 (d, J = 8.6 Hz, 1H, H^6), 7.84 (d, J = 8.2 Hz, 1H, H^9), 7.79 (s, ^{195}Pt satellites: $^3J_{Pt\text{-}H}$ = 50 Hz,1H, H^3), 7.65 (d, J = 7.9 Hz, 1H, H^{13}), 7.61 (d, J = 8.6 Hz, 1H, H^{12}), 7.58 (d, J = 8.5 Hz, 2H, H^{para}), 7.57 (d, J = 8.2 Hz, 1H, H^{10}), 7.29 (d, J = 8.6 Hz, 1H, H^{11}), 7.07 (d, J = 8.5 Hz, 1H, H^{16}), 6.56 (ddd, J = 7.2 Hz, J = 5.8 Hz, J = 1.6 Hz, 1H, $H^{5'}$), 6.51 (ddd, J = 8.1 Hz, J = 7.2 Hz, J = 1.8 Hz, 1H, $H^{4'}$), 6.32 (ddd, J = 8.5 Hz, J =

6.9 Hz, J = 1.3 Hz, 1H, H^{15}), 6.10 (ddd, J = 7.9 Hz, J = 6.9 Hz, J = 1.1 Hz, 1H, H^{14}), 5.55 (ddd, J = 8.1 Hz, J = 1.6 Hz, J = 0.6 Hz, 1H, $H^{3'}$), 4.06 (s, 3H, −OCH_3), 3.71 (s, 3H, −SOCH_3), 2.58 (s, 3H, ArCH_3). ^{13}C{^{1}H} NMR (100 MHz, $CDCl_3$), δ = 167.1 ($C^{2'}$), 155.9 (C^4), 147.7 ($C^{6'}$), 144.6 (C^2), 143.3 (C^{para}), 141.3 (C^{ipso}), 135.8 ($C^{4'}$), 134.6 (C^1), 132.1 (C^{8a}), 131.9 (C^{12a}), 131.8 (C^{6a}), 131.2 (C^{10a}), 129.9 (C^{meta}), 128.5 (C^{16a}), 128.1 (C^{12}), 128.0 (C^{13} and C^{16b}), 127.6 (C^{16e}), 127.4 (C^8), 127.1 (C^{16c}), 127.0 (C^7), 126.4 (C^{ortho}), 126.4 (C^{10}), 126.1 (C^9), 125.5 (C^{16}), 125.3 (C^{14}), 125.1 (C^{11}), 124.2 (C^6 and C^{15}), 123.4 (C^{16d}), 122.9 (C^{4a}), 121.7 (C^5),118.1 ($C^{5'}$), 118.1 ($C^{3'}$), 111.4 (C^3), 56.3 (−OCH_3), 49.8 (−SOCH_3), 21.7 (ArCH_3). $[\alpha]_D^{23}$ = +2350, $[\phi]_D^{23}$ = +19210 (CH_2Cl_2, 10^{-4} mol·L^{-1}). Elemental analysis, calcd. (%) for $C_{40}H_{30}ClNO_2PtS$: C 58.64, H 3.69; found : C 58.60, H 3.71.

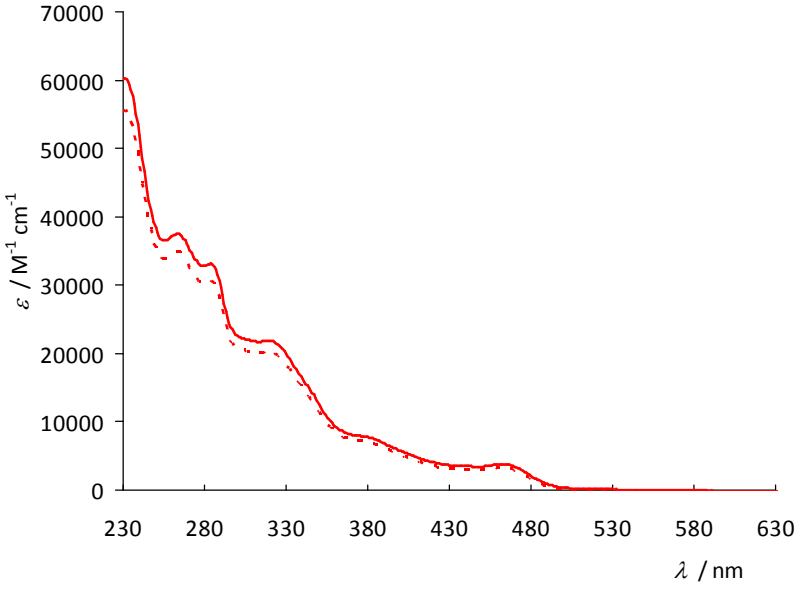

Figure S1. UV-vis spectra of (P,R_S)-**2a**^{1} (red plain lines) and (M,R_S)-**2a**^{2} (red dashed lines) diastereomers (CH_2Cl_2, 10^{-5} mol L^{-1})

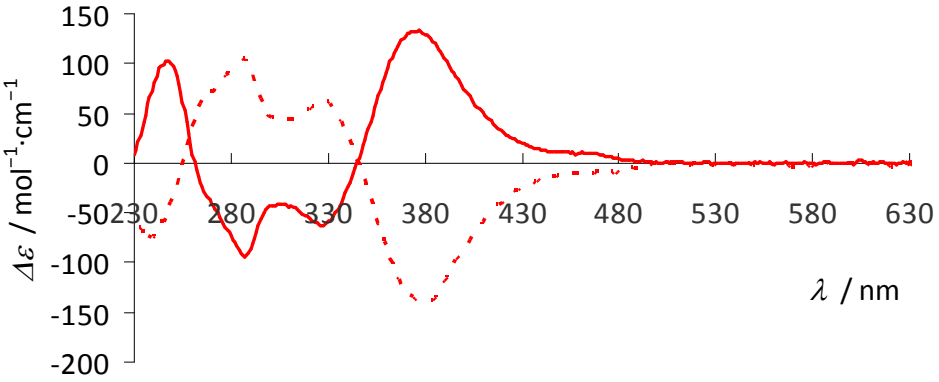

Figure S2. ECD spectra of (P,R_S)-**2a**^{1} (red plain lines) and (M,R_S)-**2a**^{2} (red dashed lines) diastereomers (CH_2Cl_2, 10^{-5} mol L^{-1})

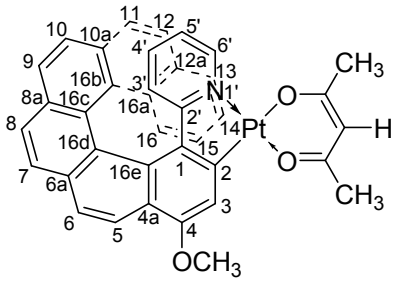

Enantiomeric complexes *P*-3a and *M*-3a. A mixture of platinum(II) complex **(*P*,R_S)-2a**[2] (74.2 mg, 0.1 mmol), sodium 2,4-pentanedionate (12.8 mg 0.105 mmol) in 10 mL toluene was refluxed for 18 hours under argon. The cooled reaction mixture was concentrated in vacuum and was purified by column chromatography (silica, chloroform) to afford the product (68.3 mg, 95%) as a yellow solid. $[\alpha]_D^{23}$ = +3091, $[\phi]_D^{23}$ = +22500 (±5%) (CH_2Cl_2, 10^{-4} mol·L^{-1}). The same procedure applied to **(*M*,R_S)-2a**[1] afforded *M*-**3a**. $[\alpha]_D^{23}$ = -3111, $[\phi]_D^{23}$ = -22650 (±5%) (CH_2Cl_2, 10^{-4} mol·L^{-1}). ^{1}H NMR (400 Hz, C*D*Cl_3), δ 8.38 (d, J = 8.5 Hz, 1H, H^5), 8.23 (ddd, J = 5.8 Hz, J =1.7 Hz, J = 0.6 Hz, ^{195}Pt satellites: $^3J_{Pt\text{-}H}$ = 35 Hz, 1H, $H^{6'}$), 8.00 (AB system, J =8.3 Hz, 1H, H^7), 7.99 (AB system, J = 8.3 Hz, 1H, H^8), 7.92 (d, J = 8.2 Hz, 1H, H^9), 7.84 (d, J = 8.5 Hz, 1H, H^6), 7.74 (d, J = 8.0 Hz, 1H, H^{13}), 7.65 (d, J = 8.2 Hz, 1H, H^{10}), 7.48 (d, J = 8.5 Hz, 1H, H^{12}), 7.31 (d, J = 8.5 Hz, 1H, H^{11}) 7.21 (d, J = 8.5 Hz, 1H, H^{16}) 7.16 (ddd, J = 8.0 Hz, J = 6.9 Hz, J = 1.1 Hz, 1H, H^{14}), 6.91 (s, ^{195}Pt satellites: $^3J_{Pt\text{-}H}$ = 46 Hz,1H, H^3), 6.61 (ddd, J = 8.5 Hz, J = 6.9 Hz, J = 1.3 Hz, 1H, H^{15}), 6.51 (ddd, J = 8.3 Hz, J = 7.3 Hz, J = 1.7 Hz, 1H, $H^{4'}$), 6.42 (ddd, J = 7.3 Hz, J = 5.8 Hz, J = 1.5 Hz, 1H, $H^{5'}$), 5.49 (ddd, J = 8.3 Hz, J = 1.5 Hz, J = 0.6 Hz, 1H, $H^{3'}$), 5.42 (s, 1H, −CH^{Acac}),4.12 (s, 3H, −OCH_3), 2.00 (s, 3H, −CH_3^{Acac}), 1.98 (s, 3H, −CH_3^{Acac}). ^{13}C{^{1}H} NMR (100 MHz, C*D*Cl_3), δ 185.5 (*C*=O), 183.8 (*C*=O), 168.2 ($C^{2'}$), 155.0 (C^4), 145.3 ($C^{6'}$), 144.6 (C^2), 134.35 ($C^{4'}$), 134.3 (C^1), 132.2 (C^{6a}), 131.9 (C^{12a}), 131.8 (C^{8a}), 131.2 (C^{10a}), 128.7 (C^{16a}), 128.2 (C^{16b}), 127.9 (C^{12}), 127.6 (C^{13} and C^{16e}), 127.2 (C^{16c}), 127.2 (C^8), 126.9 (C^7), 126.3 (C^9), 126.2 (C^{10}), 125.7 (C^{14}), 125.5 (C^{16}), 124.5 (C^{15}), 122.9 (C^6), 122.8 (C^{16d}), 122.6 (C^{4a}), 122.2 (C^5), 118.0 ($C^{3'}$), 117.8 ($C^{5'}$), 107.7 (C^3), 102.2 (−*C*H^{Acac}), 56.1 (−O*C*H$_3$), 28.3 (−*C*H$_3^{Acac}$), 27.4 (−*C*H$_3^{Acac}$). Elemental analysis, calcd. (%) for $C_{37}H_{27}NO_3Pt$: C 60.99, H 3.73; found : C 60.93, H 3.76.

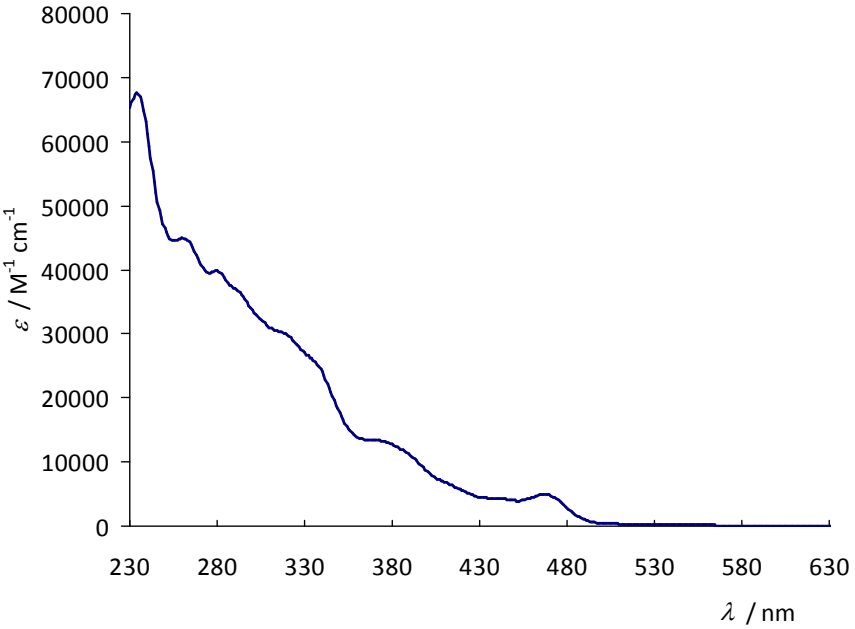

Figure S3. UV-vis spectrum of **3a** (CH_2Cl_2, 10^{-5} mol L^{-1})

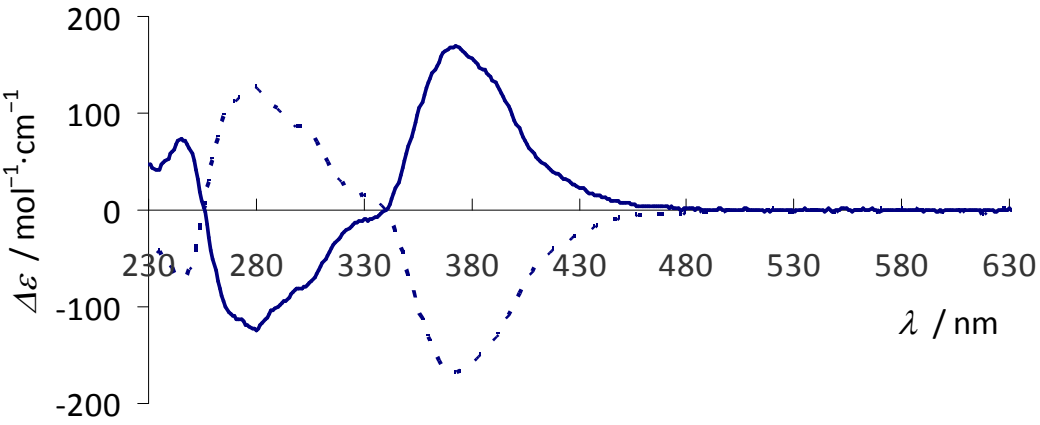

Figure S4. ECD spectra of *P*-**3a** (blue plain lines) and *M*-**3a** (blue dashed lines) (CH_2Cl_2, 10^{-5} mol L^{-1})

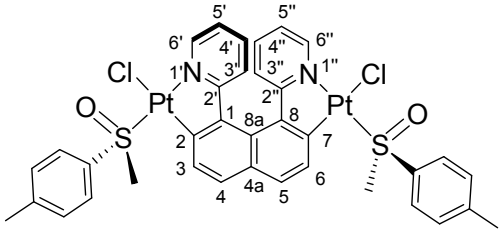

(M,R_S,R_S)-**2b**^{1}

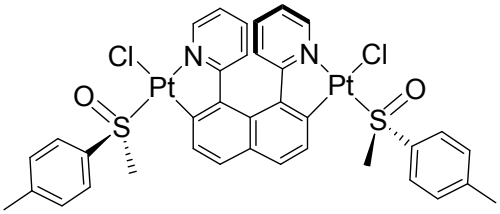

(P,S_S,S_S)-**2b**^{1}

(1,8-di(pyriden-2-yl)naphthalenato-($N^{1'}$,C^{2}),($N^{1''}$,C^{7}))bis((methyl-(*p*-tolyl)sulfoxide-*S*)platinum(II)chloride) 2b^{1,2}

A suspension of 1,8-di(pyriden-2-yl)naphthalene[2] (85 mg, 0.30 mmol), (R_S,R_S)-bis(methyl-(*p*-tolyl)sulfoxide-*S*)platinum(II) chloride (370 mg, 0.64 mmol) and Na_2CO_3 (100 mg, 0.94 mmol) in 10 mL toluene was refluxed under argon overnight, and concentrated in vacuo. Column chromatography (silica gel, $V_{heptane}$:$V_{ethyl\ acetate}$ = 1:1) afforded a first eluted fraction (pure (M,R_S,R_S)-**2b**^{1}, 25 mg, 8%) as a yellow powder, a second eluted fraction ((M,R_S,R_S)-**2b**^{1} and (P,R_S,R_S)-**2b**^{1} 11:9, 82 mg, 26%) and a third eluted fraction ((M,R_S,R_S)-**2b**^{1} and (P,R_S,R_S)-**2b**^{1}, 1:3, 65 mg, 21%). The third eluted fraction was dissolved in a minimum solvent of $CHCl_3$ and precipitated with heptane/$CHCl_3$ (3:1) to afford (P,R_S,R_S)-**2b**^{1} (48 mg, 15%) as a yellow powder. The complex mixture could be recycled and resolved again, yielding finally 50 mg (33% yield for resolution step, 16% global yield) of (M,R_S,R_S)-**2b**^{1}, $[\alpha]_D^{23}$ = -1123, $[\phi]_D^{23}$ = -11790 (CH_2Cl_2, 10^{-4} mol·L^{-1}). Elemental analysis, calcd. (%) for $C_{36}H_{32}Cl_2N_2O_2Pt_2S_2$: C 41.19, H 3.07; found : C 40.82, H 3.23.

The same procedure starting from (R_S,R_S)-bis(methyl-(*p*-tolyl)sulfoxide-*S*)platinum(II) chloride afforded (P,S_S,S_S)-**2b**^{1}, $[\alpha]_D^{23}$ = +1133, $[\phi]_D^{23}$ = +11890 (CH_2Cl_2, 10^{-4} mol·L^{-1}).

(P,S_S,S_S)-**2b**^{1}: ^{1}H NMR (400 MHz, C*D*Cl$_3$), δ 9.63 (ddd, J = 6.0 Hz, J = 1.6 Hz, J = 0.6 Hz, ^{195}Pt satellites: $^{3}J_{Pt\text{-}H}$ = 30 Hz, 2H, $H^{6'}$ and $H^{6''}$), 8.24 (d, J = 8.4 Hz, 4H, H^{ortho}), 7.70 (d, J = 8.4 Hz, 2H,H^{3} and H^{6}), 7.57 (ddd, J = 8.3 Hz, J = 7.2 Hz,J = 1.6 Hz, 2H, $H^{3'}$ and $H^{3''}$), 7.51 (ddd, J = 8.3 Hz, J = 7.2 Hz, J = 1.6 Hz, 2H, $H^{4'}$ and $H^{4''}$), 7.43 (d, J = 8.4 Hz, 4H, H^{meta}), 7.38 (d, J = 8.4 Hz, 2H, H^{4} and H^{5}), 7.05 (ddd, J = 7.2 Hz, J = 6.0 Hz, J = 1.5 Hz, 2H, $H^{5'}$ and $H^{5''}$), 3.78 (s, 6H, −SOCH_3), 2.47 (s, 6H, ArCH_3). ^{13}C{^{1}H } NMR (100 MHz, CDCl$_3$), δ = 166.8 ($C^{2'}$ and $C^{2''}$), 149.8 ($C^{6'}$ and $C^{6''}$), 148.9 (C^{2} and C^{7}), 143.9 (C^{para}), 140.6 (C^{ipso}), 139.5 ($C^{4'}$ and $C^{4''}$), 137.2 (C^{1} and C^{8}), 131.7 (C^{3} and C^{6}),131.6 (C^{4a}), 130.9 (C^{4} and C^{5}), 130.3 (C^{meta}), 126.0 (C^{ortho}), 125.6 (C^{8a}), 123.3 ($C^{3'}$ and $C^{3''}$), 120.5 ($C^{5'}$ and $C^{5''}$), 49.8 (−SO*C*H$_3$), 21.6 (Ar*C*H$_3$).

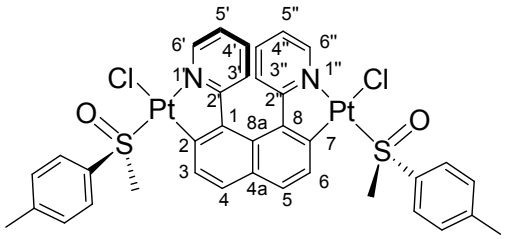

(*M*,S_S,S_S)-**2b²**

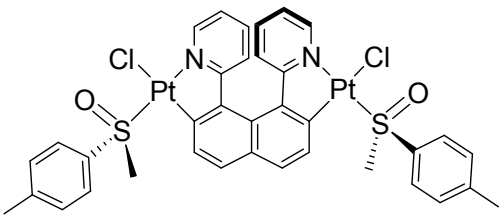

(*P*,R_S,R_S)-**2b²**

A suspension of 1,8-di(pyriden-2-yl)naphthalene **1b** (85 mg 0.30 mmol), (S_S,S_S)-bis(methyl-(*p*-tolyl)sulfoxide-*S*)platinum(II) chloride (413 mg, 0.72 mmol) and Na_2CO_3 (254 mg, 2.4 mmol) in 10 mL toluene was refluxed under argon overnight, and concentrated in vacuo. Short column chromatography (silica gel, ethyl acetate) afforded the complex (154 mg, 49%, 1:1.5 mixture of (*P*,S_S,S_S)-**2b¹** and (*M*,S_S,S_S)-**2b²**). The product was precipitated in heptane/$CHCl_3$ (3:1) to afford (*M*,S_S,S_S)-**2b²** (55 mg, 17% global yield) as a yellow powder. $[\alpha]_D^{23}$ = -863, $[\phi]_D^{23}$ = -9060 (CH_2Cl_2, 10^{-4} mol·L^{-1}). Elemental analysis, calcd. (%) for $C_{36}H_{32}Cl_2N_2O_2Pt_2S_2$: C 41.19, H 3.07; found : C 40.90, H 3.23.

The same procedure starting from (R_S,R_S)-bis(methyl-(*p*-tolyl)sulfoxide-*S*)platinum(II) chloride afforded (*P*,R_S,R_S)-**2b²**. $[\alpha]_D^{23}$ = +916, $[\phi]_D^{23}$ = +9615 (CH_2Cl_2, 10^{-4} mol·L^{-1}).

(*P*,R_S,R_S)-**2b²**: ^{1}H NMR (400 MHz, C*D*Cl_3), δ 9.58 (dd, *J* = 5.9 Hz, *J* = 1.6 Hz, ^{195}Pt satellites: $^3J_{Pt\text{-}H}$ = 30 Hz, 2H, $H^{6'}$ and $H^{6''}$), 8.17 (d, *J* = 8.5 Hz, 2H, H^3 and H^6), 8.06 (d, *J* = 8.4 Hz, 4H, H^{ortho}), 7.47 (ddd, *J* = 8.1 Hz, *J* = 7.4 Hz, *J* = 1.6 Hz, 2H, $H^{4'}$ and $H^{4''}$), 7.38 (d, *J* = 8.5 Hz, 2H, H^4 and H^5),7.32 (d, *J* = 8.1 Hz, 2H, $H^{3'}$ and $H^{3''}$), 7.29 (d, *J* = 8.4 Hz, 4H, H^{meta}), 7.03 (ddd, *J* = 7.4 Hz, *J* = 5.9 Hz, *J* = 1.3 Hz, 2H, $H^{5'}$ and $H^{5''}$), 3.77 (s, 6H, −SOCH_3), 2.36 (s, 6H, ArCH_3). ^{13}C{^{1}H } NMR (100 MHz, $CDCl_3$), δ = 166.8 ($C^{2'}$ and $C^{2''}$), 149.9 ($C^{6'}$ and $C^{6''}$), 148.0 (C^2 and C^7), 143.6 (C^{para}), 140.6 (C^{ipso}), 139.3 ($C^{4'}$ and $C^{4''}$), 136.9 (C^1 and C^8), 131.6 (C^{4a}), 130.8 (C^4 and C^5), 130.7 (C^3 and C^6), 130.1 (C^{meta}), 125.8 (C^{8a}), 125.6 (C^{ortho}),123.4 ($C^{3'}$ and $C^{3''}$), 120.5 ($C^{5'}$ and $C^{5''}$), 49.4 (−SOCH_3), 21.5 (ArCH_3).

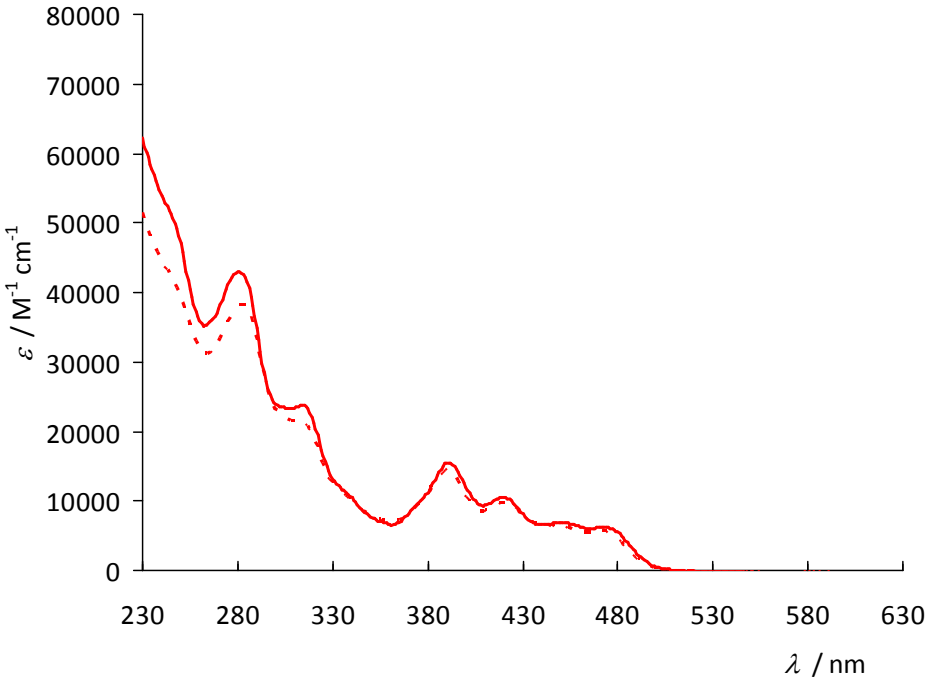

Figure S5. UV-vis spectra of (*M*,R_S,R_S)-**2b**^{1} (red plain lines) and (*P*,R_S,R_S)-**2b**^{2} (red dashed lines) diastereomers (CH_2Cl_2, 10^{-5} mol L^{-1}).

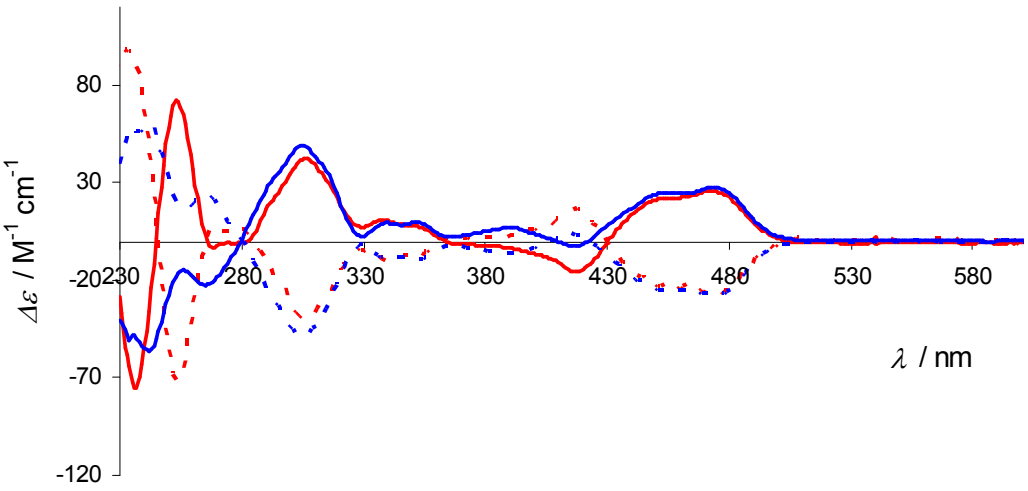

Figure S6. ECD spectra of (*P*,S_S,S_S)-**2b**^{1} (blue plain lines) and (*M*,R_S,R_S)-**2b**^{1} (blue dashed lines), (*P*,R_S,R_S)-**2b**^{2} (red plain lines) and (*M*,S_S,S_S)-**2b**^{2} (red dashed lines) diastereomers (CH_2Cl_2, 10^{-5} mol L^{-1}).

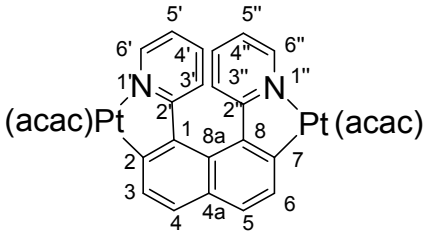

A mixture of (P,R_S,R_S)-**2b**^{2} (21 mg) and sodium 2,4-pentanedionate (5.9 mg) in 3 mL toluene was refluxed for 2 hours under argon. The cooled reaction mixture was concentrated in vacuo and was purified by column chromatography (silica gel, CH_2Cl_2) to afford *P*-**3b** (13 mg, 75%) as a yellow solid.

A mixture of (M,S_S,S_S)-**2b**^{2} (22 mg) and sodium 2,4-pentanedionate (5.9 mg) in 3 mL toluene was refluxed for 2 hours under argon. The cooled reaction mixture was concentrated in vacuum and was purified by column chromatography (silica gel, CH_2Cl_2) to afford *P*-**3b** (13 mg, 71%) as a yellow solid.

^{1}H NMR (400 MHz, C*D*Cl$_3$), δ 8.92 (ddd, J = 5.8 Hz, J = 1.6 Hz, J = 0.6 Hz, ^{195}Pt satellites: $^3J_{\text{Pt-H}}$ = 34 Hz, 2H, $H^{6'}$ and $H^{6''}$), 7.73 (d, J = 8.1 Hz, 2H,H^3 and H^6), 7.64 (d, J = 8.1 Hz, 2H, H^4 and H^5), 7.32 (ddd, J = 8.3 Hz, J = 7.3 Hz, J = 1.6 Hz, 2H, $H^{4'}$ and $H^{4''}$), 7.18 (ddd, J = 8.3 Hz, J = 1.2 Hz, J = 0.6 Hz, 2H, $H^{3'}$ and $H^{3''}$), 6.90 (ddd, J = 7.3 Hz, J = 5.8 Hz, J = 1.2 Hz, 2H, $H^{5'}$ and $H^{5''}$), 5.53 (s, 2H, −CH^{Acac}), 2.06 (s, 6H, −CH_3^{Acac}), 2.05 (s, 6H, −CH_3^{Acac}). ^{13}C{^{1}H } NMR (100 MHz, C*D*Cl$_3$), δ 186.1 (*C*=O), 184.8 (*C*=O), 168.8 ($C^{2'}$ and $C^{2''}$), 147.2 ($C^{6'}$ and $C^{6''}$), 146.3 (C^2 and C^7), 136.9 ($C^{4'}$ and $C^{4''}$), 135.8 (C^1 and C^8), 131.5 (C^{4a}), 130.3 (C^4 and C^5), 127.1 (C^3 and C^6), 126.1 (C^{8a}), 123.3 ($C^{3'}$ and $C^{3''}$), 119.7 ($C^{5'}$ and $C^{5''}$), 102.8 (−*C*H$^{\text{Acac}}$), 28.4 (−*C*H$_3^{\text{Acac}}$), 27.4 (−*C*H$_3^{\text{Acac}}$). Elemental analysis, calcd. (%) for $C_{30}H_{26}N_2O_4Pt_2$: C 41.48, H 3.02; found : C 41.49, H 3.03.

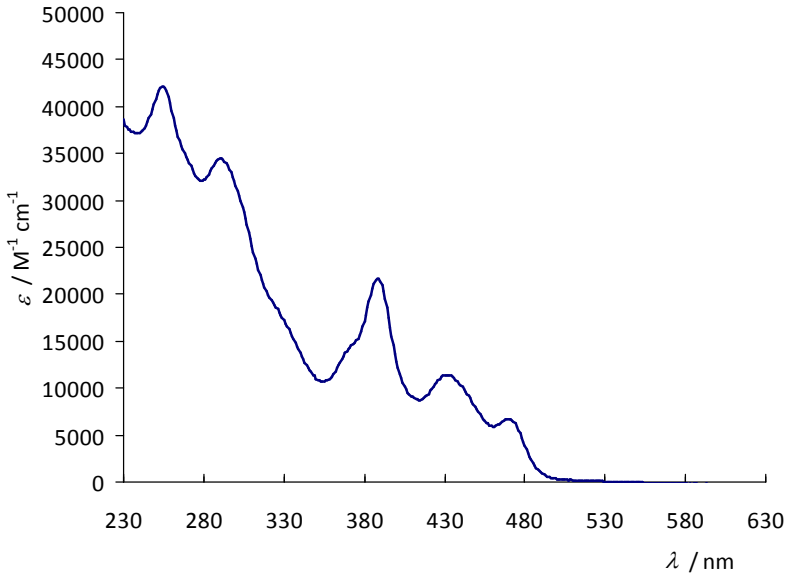

Figure S7. UV-vis spectrum of **3b** (CH_2Cl_2, 10^{-5} mol L^{-1})

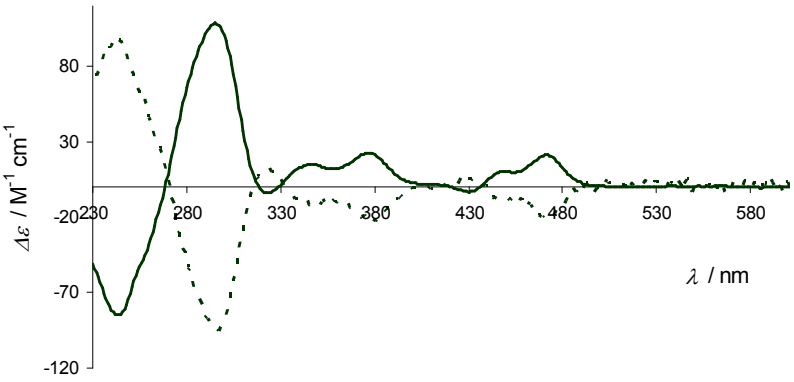

Figure S8. ECD spectra of *P*-**3b** (black plain lines) and *M*-**3b** (black dashed lines) (CH_2Cl_2, 10^{-5} mol L^{-1})

HPLC separations and analyses

Analytical chiral HPLC separation for compound **1a**

• The sample is dissolved in hexane/isopropanol/chloroform (4/1/5), injected on the chiral columns, and detected with an UV detector at 350 nm with a CD at 254 nm. The flow-rate is 1 mL/min.

Column	Mobile Phase	t1	k1	t2	k2	α	Rs
Chiralpak IA	Hexane/Isopropanol 80/20	4.71 (-)	0.57	5.63 (+)	0.88	1.53	2.37
	Hexane/Ethanol 80/20	4.91 (-)	0.64	5.98 (+)	0.99	1.56	2.90
Chiralpak IB	Hexane/Isopropanol 80/20	6.74 (-)	1.25	11.22 (+)	2.74	2.20	4.56
	Hexane/Ethanol 80/20	5.21 (-)	0.74	6.62 (+)	1.21	1.64	3.16
Chiralpak IC	Hexane/Isopropanol 80/20	11.71 (+)	2.90	13.88 (-)	3.63	1.25	1.47
	Hexane/Ethanol 80/20	7.53 (+)	1.51	7.87 (-)	1.62	1.07	0.48
Chiralpak IB	Hexane/Isopropanol/Chloroform 80/5/15	4.49 (+)	0.50	7.09 (-)	1.36	2.75	2.91
	Hexane/Isopropanol/Chloroform 70/10/20	3.88 (+)	0.29	4.95 (-)	0.65	2.22	1.85
	Hexane/Isopropanol/Chloroform 80/10/10	5.36 (+)	0.79	7.67 (-)	1.56	1.98	4.61

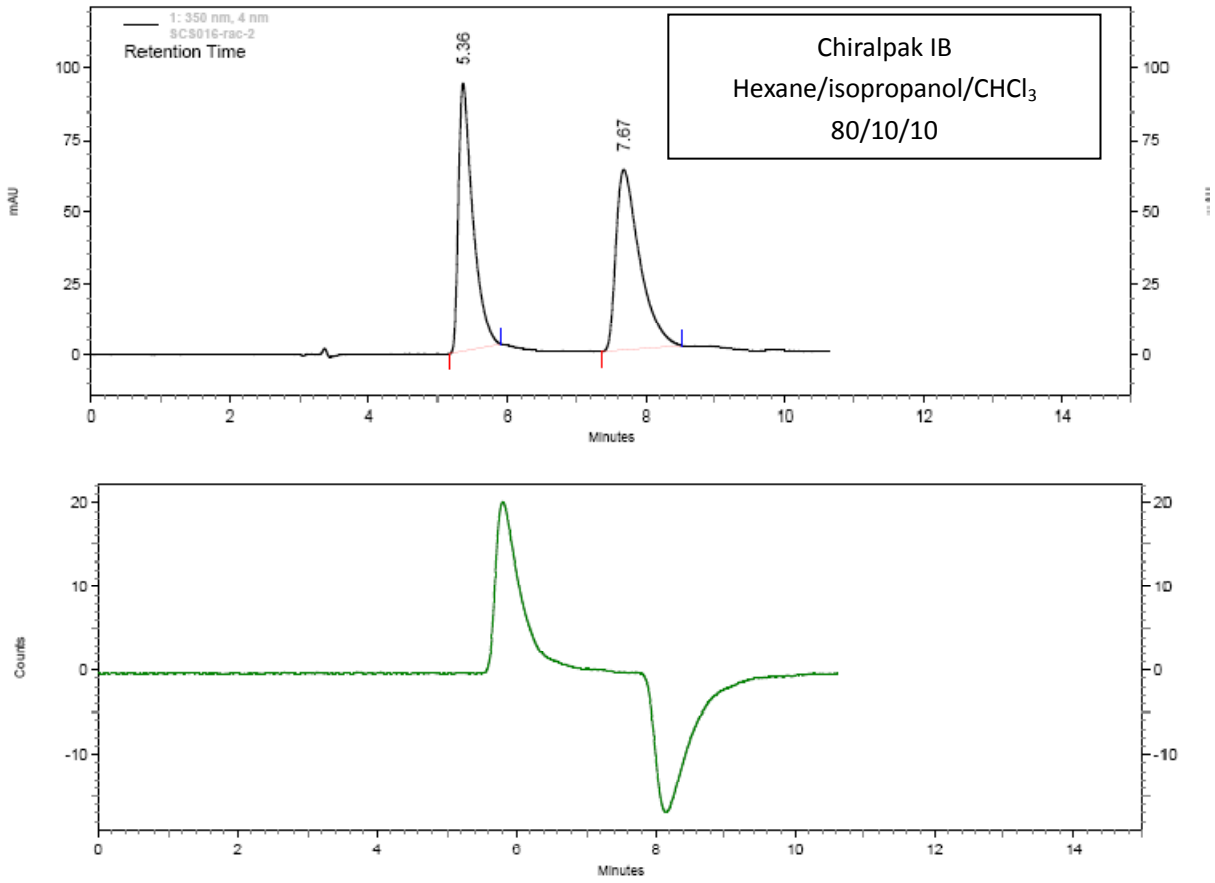

1: 350 nm, 4 nm
Results

Retention Time	Area	Area %	Capacity factor	Relative RT	Resolution (USP)
5.36	5481081	47.52	0.79	1.00	0.00
7.67	6052572	52.48	1.56	1.98	4.61
Totals	11533653	100.00			

Semi-preparative separation for compound **1a** :

• Sample preparation: About 148 mg of compound **1a** are dissolved in 40 mL of a mixture hexane/isopropanol/chloroform (40/10/50).

• Chromatographic conditions: Chiralpak IB (250 x 10 mm), thermostated at 30°C, hexane/isopropanol/chloroform (80/10/10) as mobile phase, flow-rate = 5 ml/min, UV detection at 350 nm.

• Injection: 40 times 1 mL, every 11 minutes.

• Collection: the first eluted enantiomer is collected between 5 and 7 minutes and the second one between 7 and 9 minutes.

• First fraction: 56 mg of the first eluted ((+)-enantiomer, CD 254 nm) $[\alpha]_D^{23}$ = +1827 (±7%), $[\phi]_D^{23}$ = +8290 (CH_2Cl_2, 2 10^{-5} mol·L^{-1}).

• Second fraction: 81 mg of the second eluted ((-)-enantiomer, CD 254 nm) $[\alpha]_D^{23}$ = -2093 (±7%), $[\phi]_D^{23}$ = -9500 (CH_2Cl_2, 8.910^{-5} mol·L^{-1}).

• Chromatograms of the collected enantiomers:

- The first eluted ((+)-enantiomer, CD 254 nm)

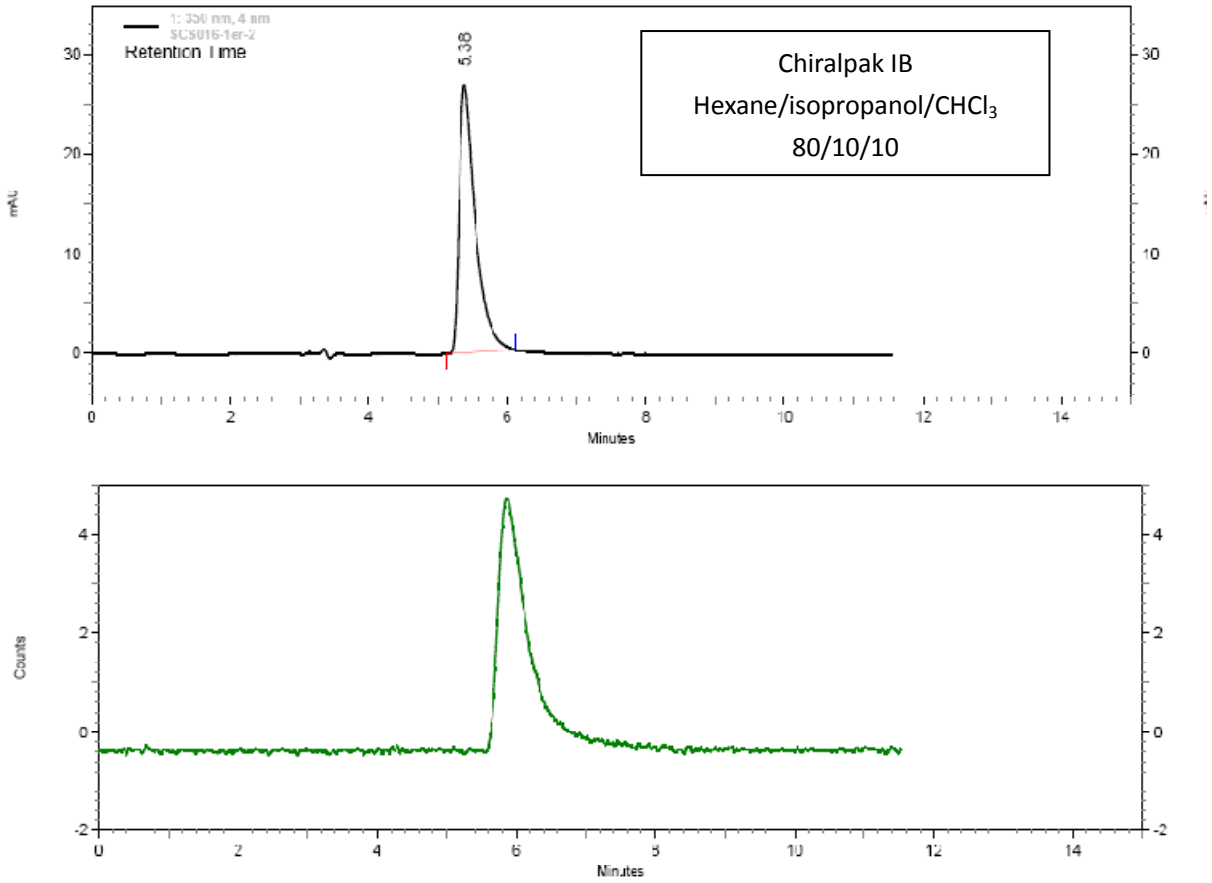

1: 350 nm, 4 nm
Results

Retention Time	Area	Area %	Capacity factor	Relative RT	Resolution (USP)
5.38	1735615	100.00	0.79	1.00	0.00
Totals	1735615	100.00			

- The second eluted ((-)-enantiomer, CD 254 nm)

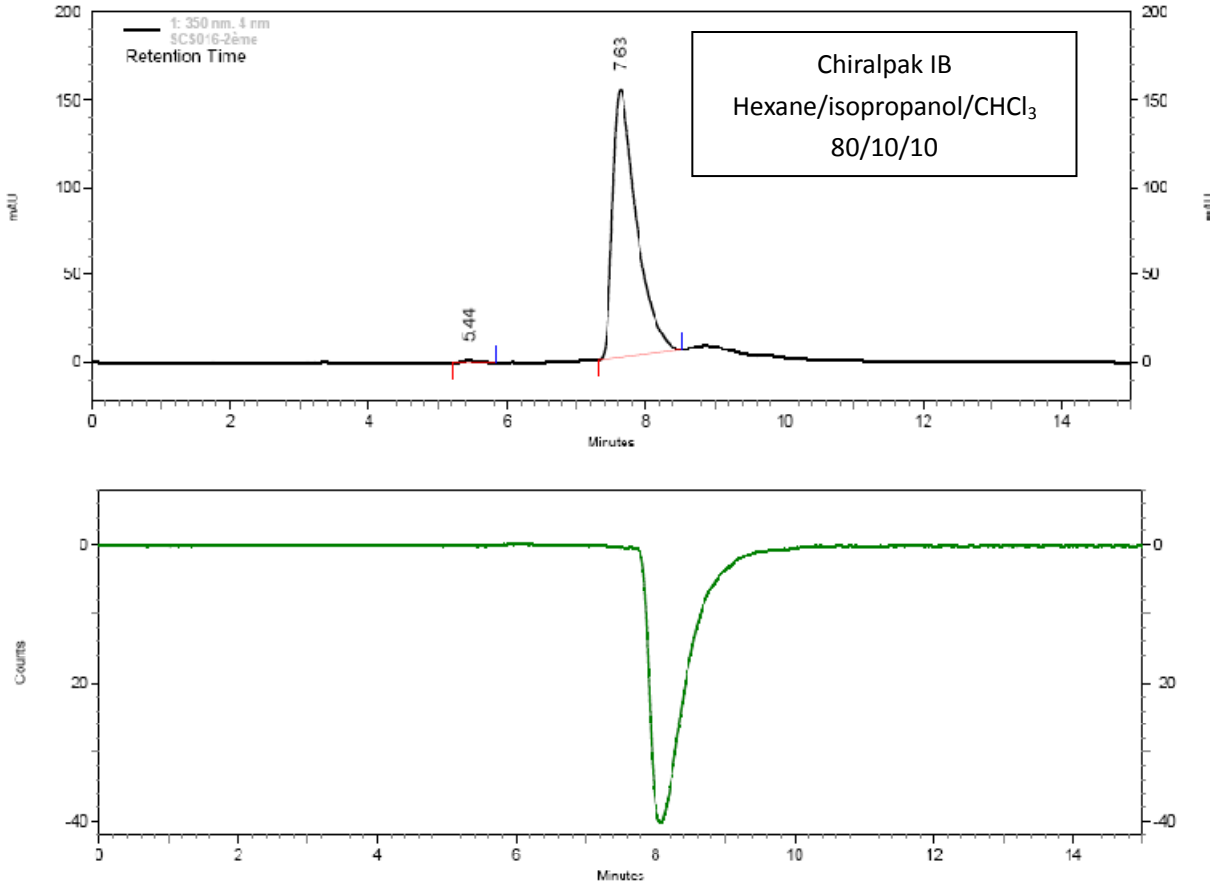

1: 350 nm, 4 nm
Results

Retention Time	Area	Area %	Capacity factor	Relative RT	Resolution (USP)
5.44	70772	0.48	0.81	1.00	0.00
7.63	14597950	99.52	1.54	1.90	4.10
Totals	14668722	100.00			

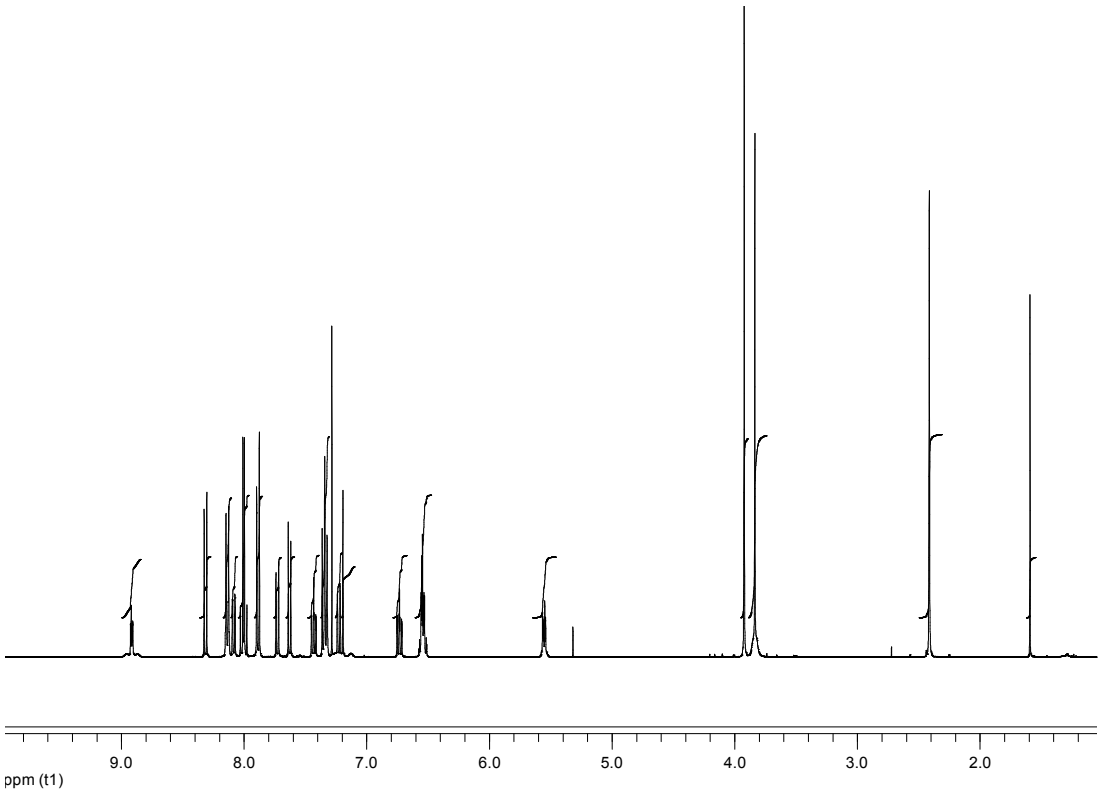

Figure S9. ^{1}H NMR (500 MHz) in $CDCl_3$ of diastereomer (P,R_S)-**2a**[2]

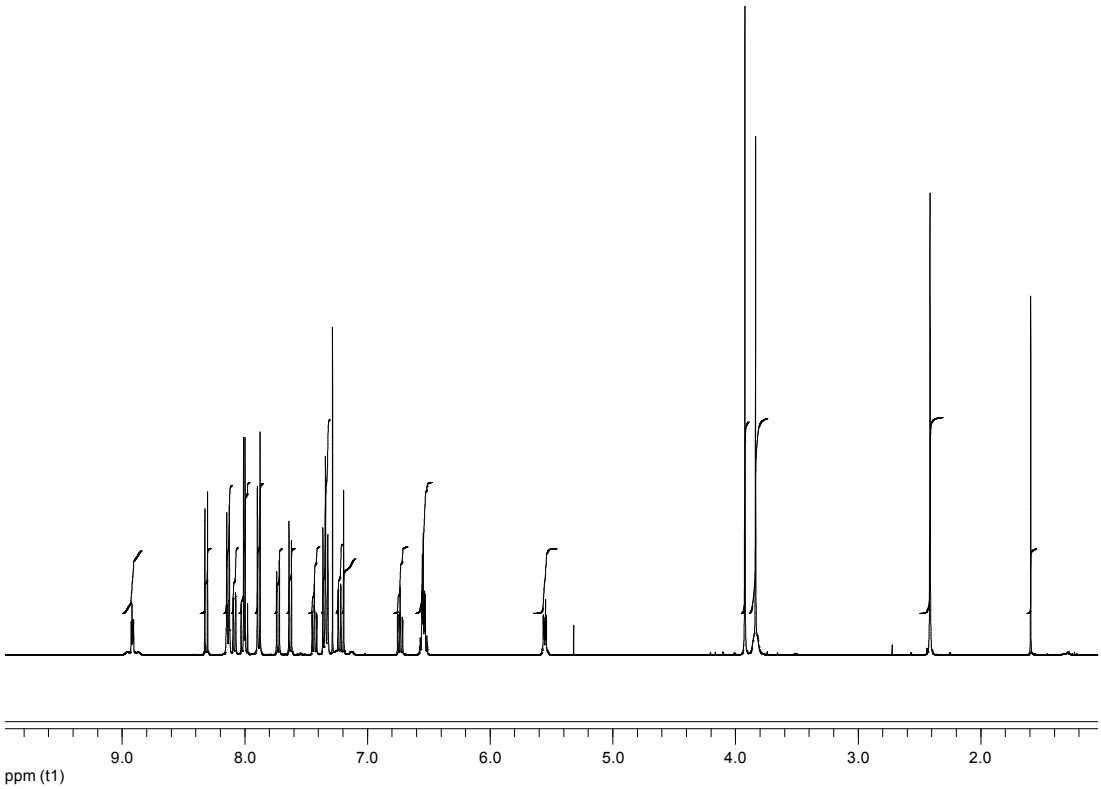

Figure S10. ^{1}H NMR (500 MHz) in $CDCl_3$ of diastereomer (M,R_S)-**2a**[1]

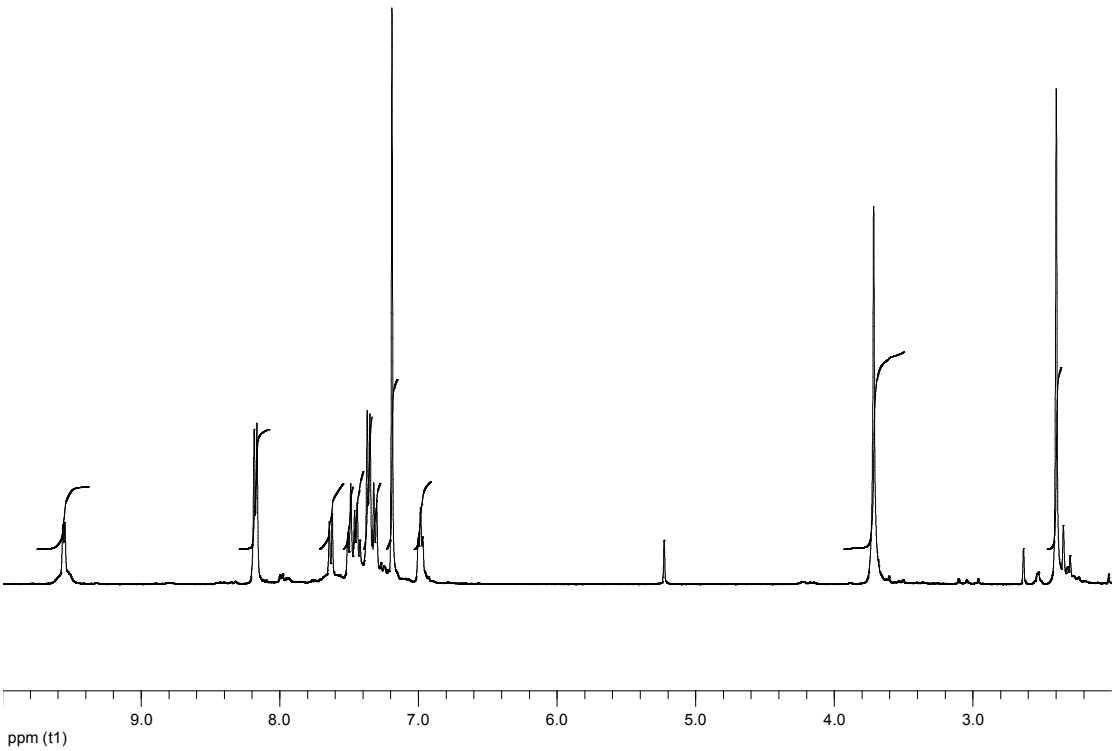

Figure S11. ^{1}H NMR (400 MHz) in $CDCl_3$ of diastereomer (P,S_S,S_S)-**2b**[1]

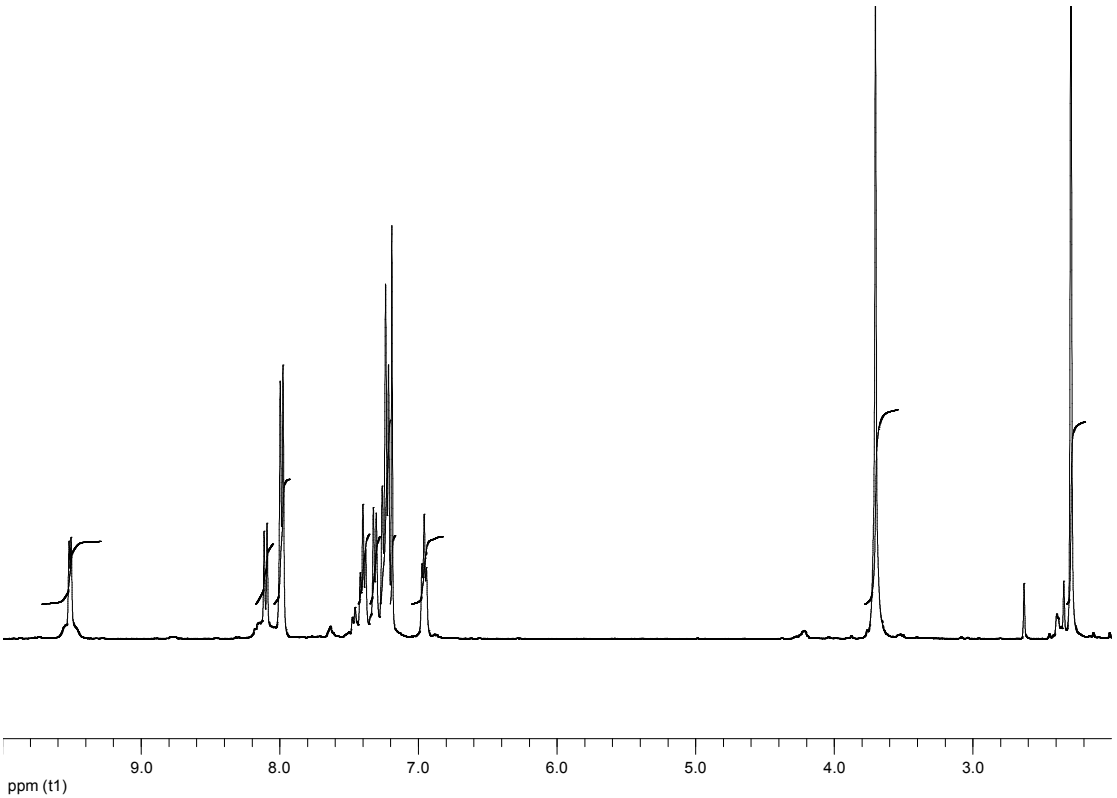

Figure S12. ^{1}H NMR (400 MHz) in $CDCl_3$ of diastereomer (P,R_S,R_S)-**2b**[2]

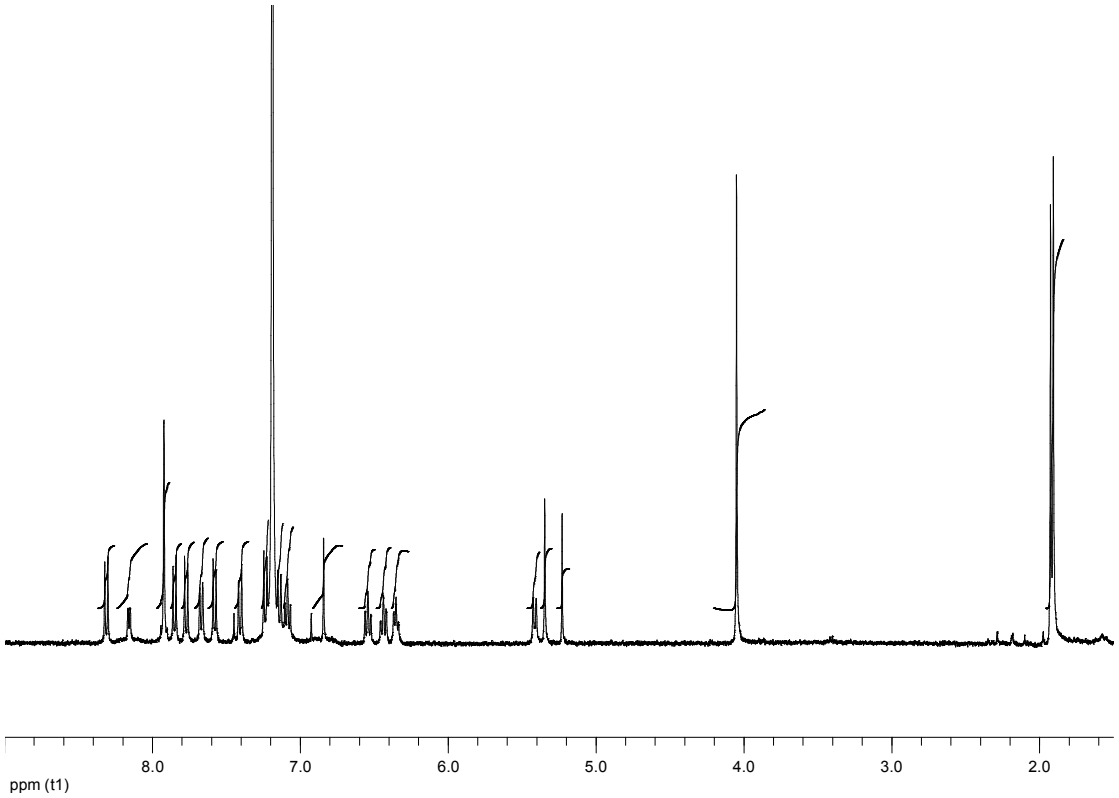

Figure S13. ^{1}H NMR (400 MHz) in $CDCl_3$ of **3a**

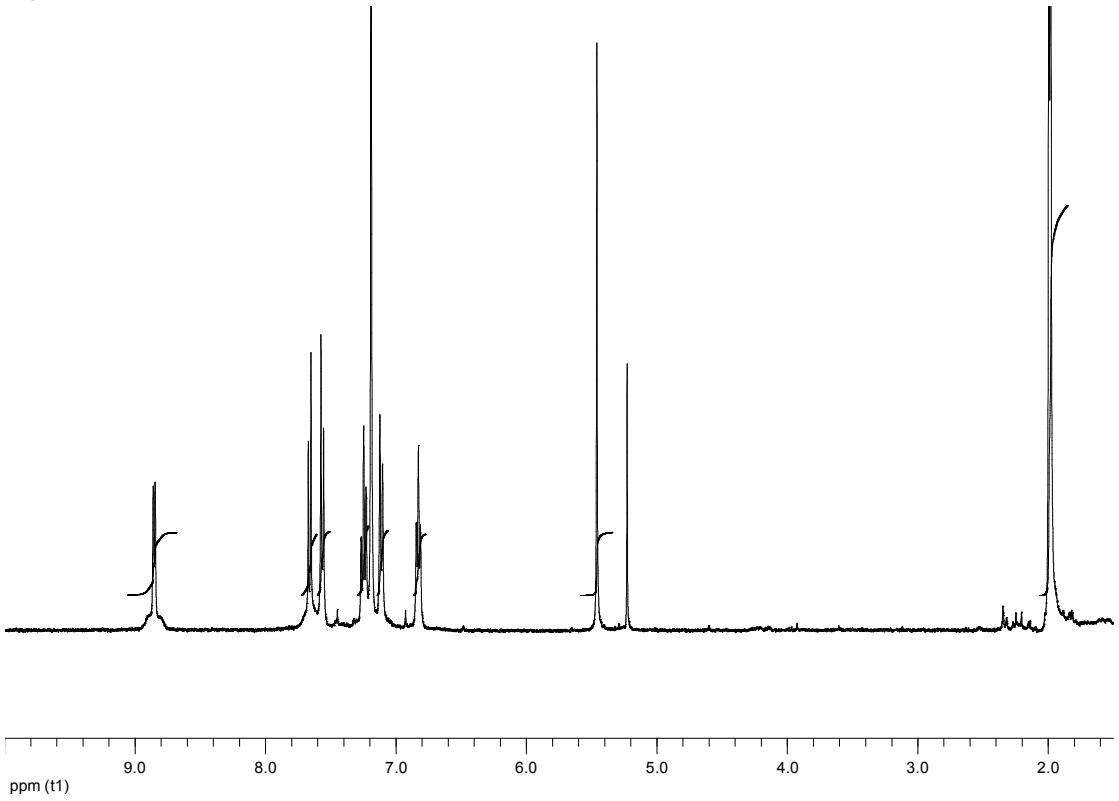

Figure S14. ^{1}H NMR (400 MHz) in $CDCl_3$ of **3b**.

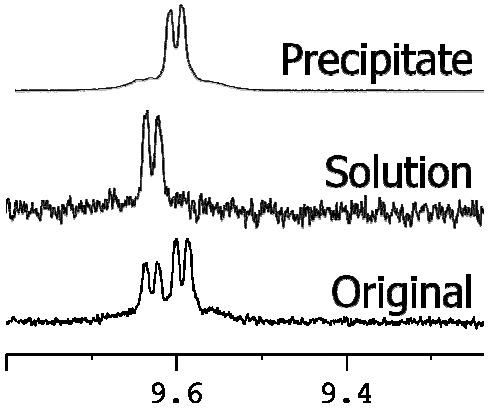

Figure S15. Composition of the crude 1:1.5 mixture of (M,R_S,R_S)-**2b**^{1} / (P,R_S,R_S)-**2b**^{2} diastereomers after double cycloplatination.

Epimerization study of (P,S_S,S_S)-2b^2

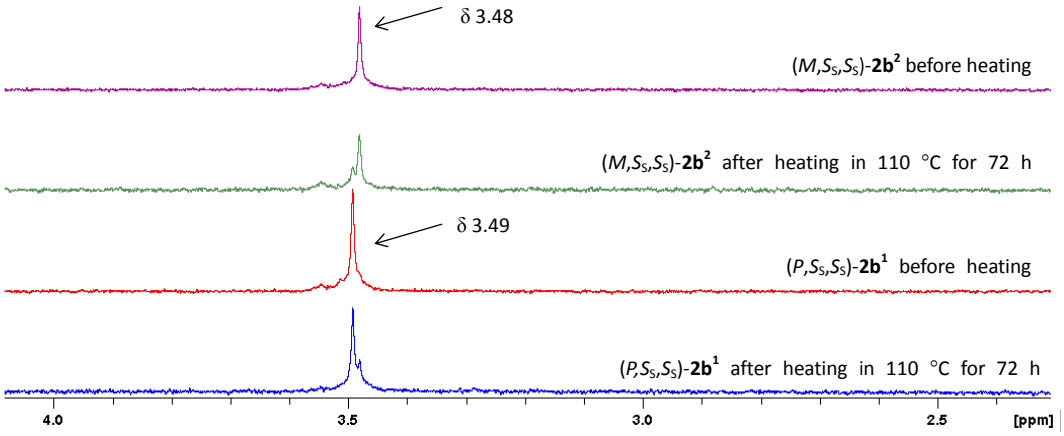

Figure S16. Evolution of ^{1}H NMR spectrum in CD_2Cl_2 of diastereomers (P,S_S,S_S)-**2b**^{1} and (M,S_S,S_S)-**2b**^{2} upon heating.

Racemization study of *P*-3b

P-**3b** (5.9 mg) was dissolved in 10.0 mL of xylene and refluxed at 100 °C and 120 °C. 1.0 mL solution was taken after 8, 16, 32 and 64 hours and experimental optical rotation (OR) was measured. The decrease of the initial OR value with time is reported below.

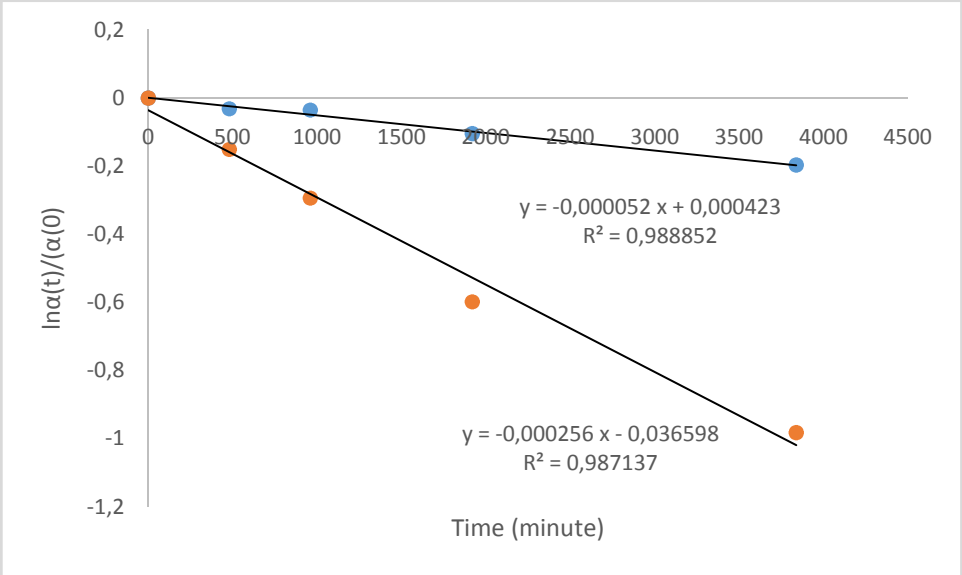

Racemization at 100 °C

$K_{racemization}$ =	4.3E-07 s^{-1}
$\Delta G_{racemization}$ =	138 kJ.mol^{-1}
	32.9 kcal.mol^{-1}
half-life time =	1.61E+06 s
	268E+04 min
	448 hours

Racemization at 120 °C

$k_{racemization}$ =	2.1E-06 s^{-1}
$\Delta G_{racemization}$=	140 kJ.mol^{-1}
	33.5 kcal.mol^{-1}
half-life time=	3.3E+05 s
	5.5E+03 min
	92 hours

X-ray diffraction data

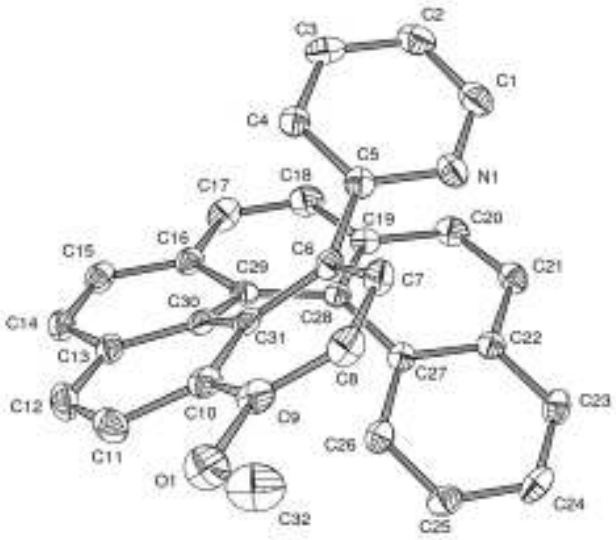

Figure S17. ORTEP diagram of ligand **1a** with ellipsoids at 50% probability.

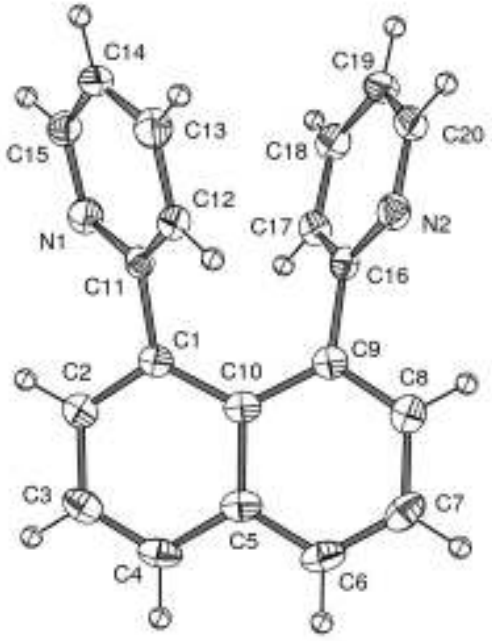

Figure S18. ORTEP diagram of ligand **1b** with ellipsoids at 50% probability.

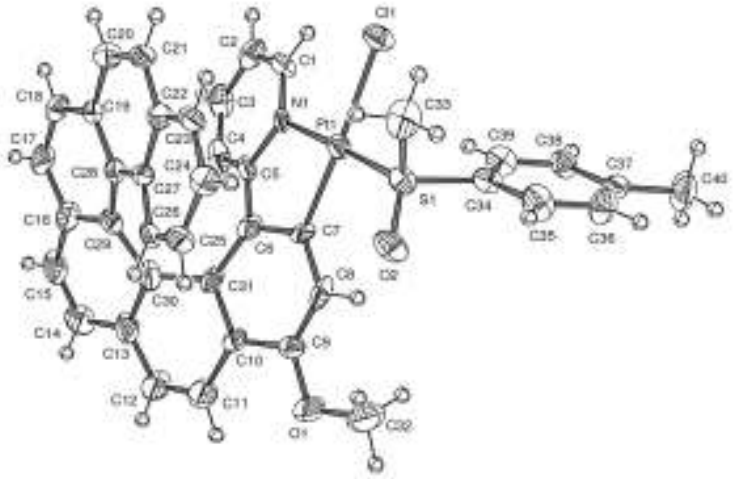

Figure S19. ORTEP diagram of complex (*M*,*R*$_S$)-**2a**[1] with ellipsoids at 50% probability.

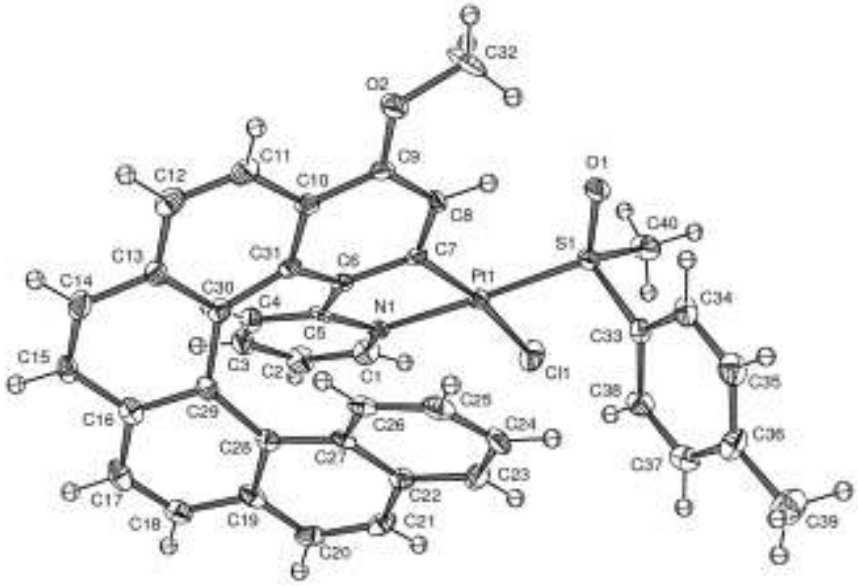

Figure S20. ORTEP diagram of complex (*P*,*R*$_S$)-**2a**[2] with ellipsoids at 50% probability.

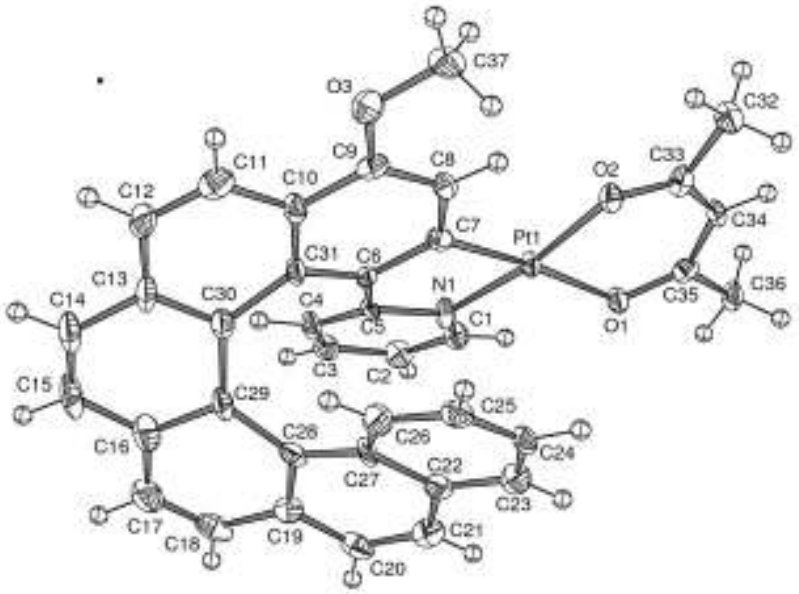

Figure S21. ORTEP diagram of complex **3a** with ellipsoids at 50% probability.

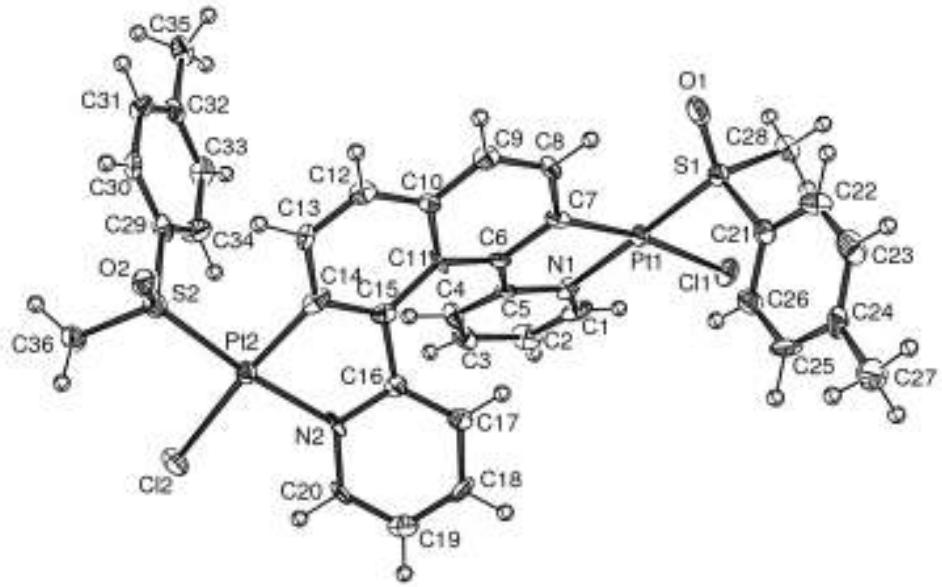

Figure S22. ORTEP diagram of complex (P,R_S,R_S)-**2b**[2] with ellipsoids at 50% probability.

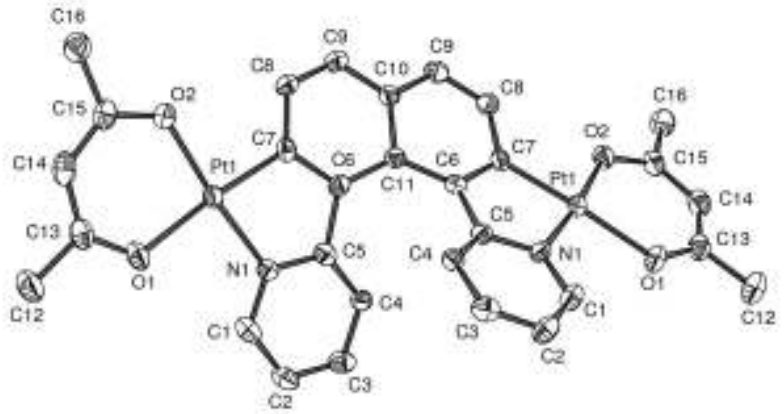

Figure S23. ORTEP diagram of complex **3b** with ellipsoids at 50% probability.

X-ray crystallographic data

	3a	**1a**	(*P*,R_S)-**2a**[2]
Empirical formula	$C_{74}H_{54}N_2O_6Pt_2$	$C_{32}H_{21}NO$	$C_{41}H_{31}Cl_4NO_2$
CCDC	869338	821845	855139
Formula weight	1457.37	435.50	938.62
Temperature (K)	120(2)	120(2)	120(2)
Wavelength (Å)	0.71073	0.71073	0.71073
Crystal system	Triclinic	Monoclinic	Orthorhombic
Space group	*P*-1	$P2_1/a$	$P2_12_12_1$
a (Å)	7.55400(10)	8.5103(8)	13.2528(2)
b (Å)	17.9390(4)	30.003(2)	14.7365(2)
c (Å)	21.6527(6)	9.1190(8)	18.3823(3)
α (°)	66.669(2)	90	90
β (°)	87.131(2)	112.410(10)	90
γ (°)	86.992(2)	90	90
Volume (Å^3)	2689.18(10)	2152.6(3)	3590.06(9)
Z	2	4	4
$\rho_{Calculated}$(g·cm^{-3})	1.800	1.344	1.737
Absorption coefficient (mm^{-1})	5.260	0.081	4.303
F(000)	1432	912	1848
Crystal size (mm)	0.208×0.072×0.065	0.24×0.14×0.12	0.24×0.21×0.18
θ range for data collection (°)	3.79 to 27.00	2.68 to 26.99	2.61 to 27.00
Limiting indices	$-9 \le h \le 9$ $-22 \le k \le 22$ $-27 \le l \le 27$	$-10 \le h \le 7$ $-38 \le k \le 38$ $-11 \le l \le 11$	$-16 \le h \le 16$ $-18 \le k \le 18$ $-23 \le l \le 23$
Reflections collected	38377	16034	50658
Reflections unique	11638 (R_{int}= 0.0658)	4703 (R_{int}= 0.0871)	7834 (R_{int}= 0.0379)
Completeness	99.1% (θ = 27.00°)	99.9% (θ = 26.99°)	99.9% (θ = 27.00°)
Absorption correction	Analytical	None	None
Max. transmission	0.76261		
Min. transmission	0.46734		
Refinement method	Full-matrix least-squares on F^2	Full-matrix least-squares on F^2	Full-matrix least-squares on F^2
Data / restraints / parameters	11638 / 0 / 727	4703 / 0 / 308	7834 / 0 / 451
Goodeness-of-fit on F^2	1.139	0.714	1.098
Final *R* indices ($I>2\sigma_I$)	R_1 = 0.0524 wR_2 = 0.1165	R_1 = 0.0423 wR_2 = 0.0599	R_1 = 0.0270 wR_2 = 0.0719
R indices (all data)	R_1 = 0.0819 wR_2 = 0.1222	R_1 = 0.1255 wR_2 = 0.0715	R_1 = 0.0310 wR_2 = 0.0729
Absolute structure parameter			−0.017(6)
Extinction coefficient		0.0030(3)	
Largest diff. peak (e·Å^3)	9.811	0.194	1.516
Largest diff. hole (e·Å^3)	−1.439	−0.185	−1.296

	(M,R_S)-**2a**[1]	**1b**	(P,R_S,R_S)-**2b**[2]
Empirical formula	$C_{40}H_{30}ClNO_2PtS$	$C_{20}H_{14}N_2$	$C_{37}H_{33}Cl_5N_2O_2Pt_2S_2$
CCDC	804094	827045	846305
Formula weight	819.25	282.33	1169.20
Temperature (K)	140(2)	140(2)	120(2)
Wavelength (Å)	0.71073	0.71073	0.71073
Crystal system	Monoclinic	Monoclinic	Orthorhombic
Space group	$P2_1$	$P2_1$	$P2_12_12_1$
a (Å)	7.7976(2)	7.5661(2)	17.2805(2)
b (Å)	13.3596(4)	12.3042(3)	17.2812(2)
c (Å)	15.2470(4)	7.9592(3)	12.5128(2)
α (°)	90	90	90
β (°)	93.639(2)	105.511(3)	90
γ (°)	90	90	90
Volume (Å^3)	1585.12(8)	713.97(4)	3736.67(9)
Z	2	2	4
$\rho_{Calculated}$(g·cm^{-3})	1.716	1.313	2.078
Absorption coefficient (mm^{-1})	4.615	0.078	7.986
F(000)	808	296	2232
Crystal size (mm)	0.23×0.19×0.12	0.25×0.22×0.21	0.147×0.061×0.047
θ range for data collection (°)	2.62 to 26.99	2.79 to 26.99	2.64 to 26.99
Limiting indices	$-9 \le h \le 9$ $-17 \le k \le 17$ $-19 \le l \le 19$	$-9 \le h \le 9$ $-15 \le k \le 14$ $-10 \le l \le 10$	$-18 \le h \le 22$ $-22 \le k \le 22$ $-15 \le l \le 14$
Reflections collected	21943	5354	28455
Reflections unique	6871 (R_{int}= 0.0913)	2967 (R_{int}= 0.0176)	8115 (R_{int}= 0.0610)
Completeness	99.9% (θ = 26.99°)	99.7% (θ = 26.99°)	99.9% (θ = 26.99°)
Absorption correction	Analytical	None	Analytical
Max. transmission	0.65230		0.73384
Min. transmission	0.45772		0.52497
Refinement method	Full-matrix least-squares on F^2	Full-matrix least-squares on F^2	Full-matrix least-squares on F^2
Data / restraints / parameters	6871 / 1 / 415	2967 / 1 / 200	8115 / 0 / 445
Goodeness-of-fit on F^2	0.927	1.001	0.796
Final R indices (I>2σ_I)	R_1 = 0.0418 wR_2 = 0.0790	R_1 = 0.0319 wR_2 = 0.0677	R_1 = 0.0312 wR_2 = 0.0397
R indices (all data)	R_1 = 0.0641 wR_2 = 0.0826	R_1 = 0.0398 wR_2 = 0.0695	R_1 = 0.0509 wR_2 = 0.0415
Absolute structure parameter	−0.017(8)	−3(2)	−0.018(5)
Extinction coefficient		0.042(3)	
Largest diff. peak (e·Å^3)	1.787	0.150	1.813
Largest diff. hole (e·Å^3)	−0.568	−0.142	−1.021

	3b
Empirical formula	$C_{30}H_{26}N_2O_4Pt_2$
CCDC number	883281
Formula weight	868.71
Temperature (K)	120(2)
Wavelength (Å)	0.71069
Crystal system	Monoclinic
Space group	*C*2/c
a (Å)	11.8533(2)
b (Å)	9.92050(10)
c (Å)	22.5187(4)
α (°)	90
β (°)	103.333(2)
γ (°)	90
Volume (Å^3)	2576.62(7)
Z	4
$\rho_{Calculated}$(g·cm^{-3})	2.240
Absorption coefficient (mm^{-1})	10.888
F(000)	1632
Crystal size (mm)	0.234×0.189×0.131
θ range for data collection (°)	2.71 to 27.00
Limiting indices	−15 ≤*h*≤ 15 −12 ≤*k*≤ 12 −28 ≤*l*≤ 28
Reflections collected	18028
Reflections unique	2815 (R_{int}= 0.0330)
Completeness	100.0% (*θ* = 27.00°)
Absorption correction	Analytical
Max. transmission	0.33631
Min. transmission	0.15490
Refinement method	Full-matrix least-squares on F^2
Data / restraints / parameters	2815 / 0 / 173
Goodeness-of-fit on F^2	1.046
Final *R* indices ($I>2\sigma_I$)	R_1 = 0.0232 wR_2 = 0.0586
R indices (all data)	R_1 = 0.0307 wR_2 = 0.0603
Absolute structure parameter	
Extinction coefficient	
Largest diff. peak (e·Å^{-3})	1.258
Largest diff. hole (e·Å^{-3})	−0.652

Photophysical measurements.

Absorption spectra were measured on a Biotek Instruments XS spectrometer, using quartz cuvettes of 1 cm path length. Steady-state luminescence spectra were measured using a Jobin Yvon FluoroMax-2 spectrofluorimeter, fitted with a red-sensitive Hamamatsu R928 photomultiplier tube. The spectral λ_{max} values in Table 1 are those obtained after correction for the wavelength dependence of the detector and emission monochromator. Samples for emission measurements at room temperature were contained within quartz cuvettes of 1 cm path length modified with appropriate glassware to allow connection to a high-vacuum line. Degassing was achieved via a minimum of three freeze-pump-thaw cycles whilst connected to the vacuum manifold; final vapour pressure at 77 K was $< 5 \times 10^{-2}$mbar, as monitored using a Pirani gauge. Luminescence quantum yields were determined using quinine sulfate in H_2SO_4(aq) as the standard for the proligands (Φ_{lum} = 0.548[4]), and $[Ru(bpy)_3]Cl_2$ in degassed aqueous solution for the complexes (Φ_{lum} = 0.042 [5]). The estimated uncertainty in Φ_{lum} is ± 20% or better.

The fluorescence lifetimes of the proligands were measured by time-correlated single-photon counting, following excitation at 374.0 nm with an EPL-375 pulsed-diode laser. The emitted light was detected at 90° using a Peltier-cooled R928 PMT after passage through a monochromator. The estimated uncertainty in the quoted lifetimes is ± 10% or better. The phosphorescence lifetimes of the proligands and of the Pt-helicenes were determined following excitation with a microsecond flashlamp, using the same detector operating in multichannel scaling mode. The bimolecular rate constants for quenching by molecular oxygen, k_Q, were determined from the lifetimes in degassed and air-equilibrated solution, taking the concentration of oxygen in CH_2Cl_2 at 0.21 atm O_2 to be 2.2 mM dm^{-3}. [6] Luminescence data at 77 K were acquired in a glass of diethyl ether / isopentane / ethanol (2:2:1 v/v), abbreviated EPA below, using 4 mm diameter quartz tubes within a home-built quartz Dewar.

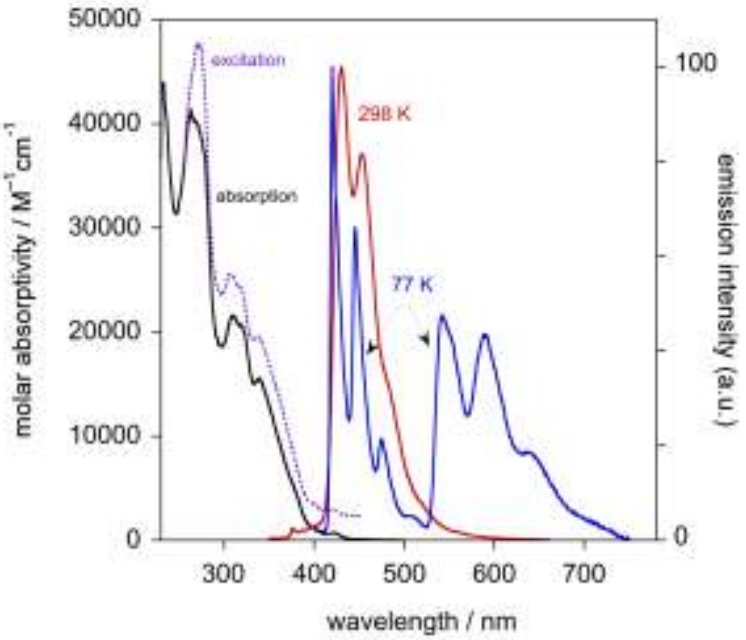

Figure S24. Absorption, excitation (λ_{em} = 446 nm) and emission spectrum of **1a** in CH_2Cl_2 at 298 K, and emission spectrum in EPA at 77 K.

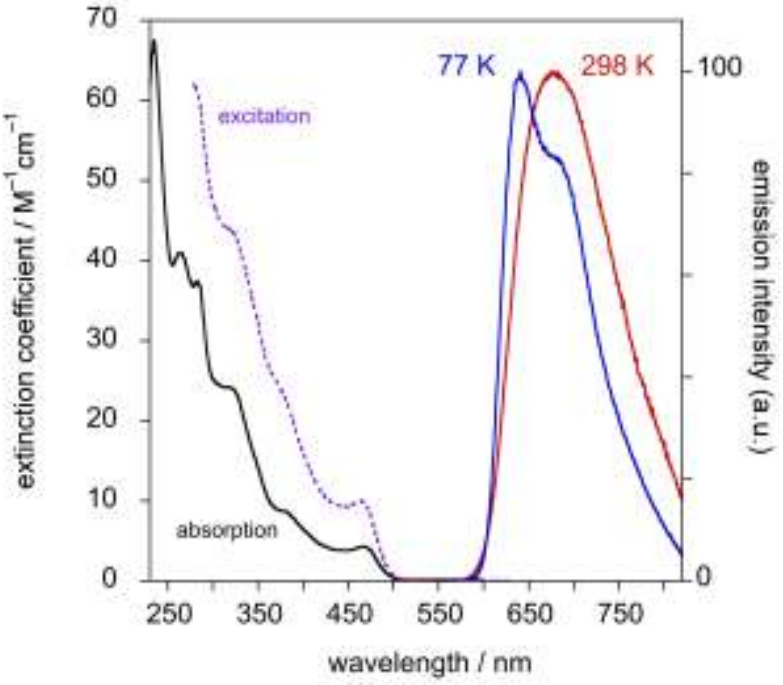

Figure S25. Absorption, excitation (λ_{em} = 660 nm) and emission spectrum of **2a**[1] in CH_2Cl_2 at 298 K, and emission spectrum in EPA at 77 K.

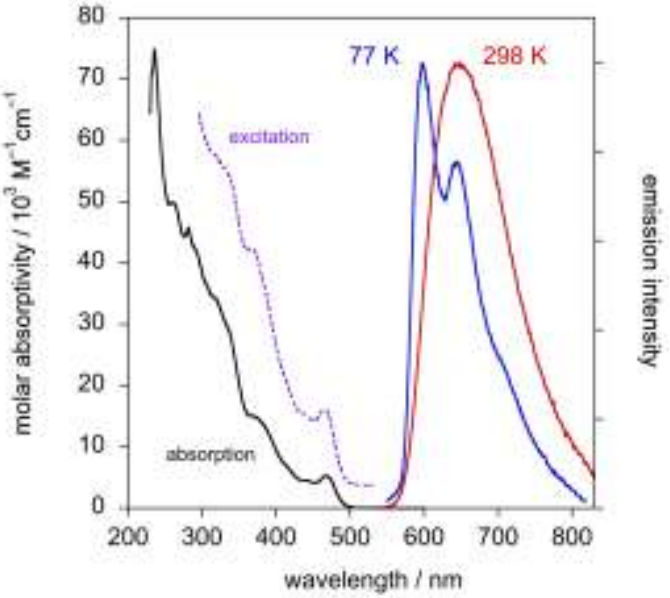

Figure S26. Absorption, excitation (λ_{em} = 670 nm) and emission spectrum of **3a** in CH_2Cl_2 at 298 K, and emission spectrum in EPA at 77 K.

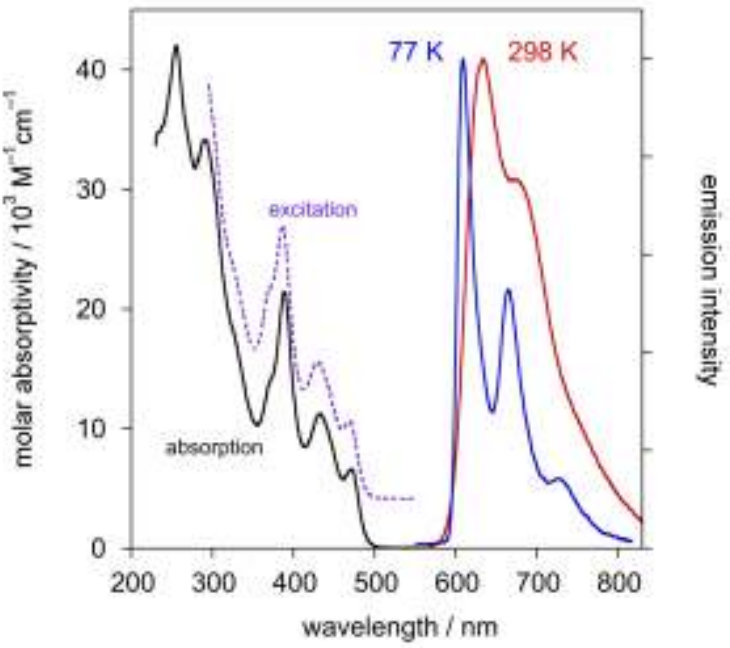

Figure S27. Absorption, excitation (λ_{em} = 630 nm) and emission spectrum of **3b** in CH_2Cl_2 at 298 K, and emission spectrum in EPA at 77 K.

CPL measurements

The circularly polarized luminescence (CPL) and total luminescence spectra were recorded on an instrument described previously,[7] operating in a differential photon-counting mode. The light source for excitation was a continuous wave 1000 W xenon arc lamp from a Spex Fluorolog-2 spectrofluorimeter, equipped with excitation and emission monochromators with dispersion of 4 nm/mm (SPEX, 1681B). To prevent artifacts associated with the presence of linear polarization in the emission,[8] a high quality linear polarizer was placed in the sample compartment, and aligned so that the excitation beam was linearly polarized in the direction of emission detection (z-axis). The key feature of this geometry is that it ensures that the molecules that have been excited and that are subsequently emitting are isotropically distributed in the plane (x,y) perpendicular to the direction of emission detection. The optical system detection consisted of a focusing lens, long pass filter, and 0.22 m monochromator. The emitted light was detected by a cooled EMI-9558B photomultiplier tube operating in photo-counting mode. All measurements were performed with quartz cuvettes with a path length of 1.0 cm.

Computational details

DFT structure optimizations were performed with the Turbomole program version 5.7.1.[9] employing the BP exchange-correlation functional[10] and a standard Turbomole split-valence basis set with one set of polarization functions for non-hydrogen atoms, SV(P).[11] A 60-electron scalar relativistic effective core potential (ECP-60) was applied for Pt.[12] The resulting optimized structures of the systems and their absolute configurations are shown in Figure S28.

TDDFT linear response optical rotation (OR) and circular dichroism (CD) calculations were performed with the BHLYP functional[13] using the SV(P)-ECP basis set. Some benchmark calculations employing two functionals with range-separated exchange,[14] CAM-B3LYP and LC-PBE0 as used in prior related works[1,15] with SV(P)-ECP and a SVPD basis set optimized for molecular response calculations[16] were carried out employing the NWChem package.[17] The optical rotation parameters were computed at the sodium *D*-line wavelength λ = 589.3 nm. The CD calculations reported here cover the 120 lowest singlet excited states (S1 to S120) for each system. The simulated spectra shown are the sums of Gaussian functions centered at the vertical excitation energies and scaled using the calculated rotatory strengths with the parameter of σ = 0.2 eV applied for the root mean square width, as previously described.[18] In some cases, chiroptical properties are given with the sign opposite that of the ones calculated because experimental data are reportedfor its optical antipode.

1a and **3a-c** were optimized in their S_1 and T_1states using TDDFT BHLYP/SVP-ECP for the purpose of calculating emission spectra. In the case of triplet states calculations, the Tamm-Dancoff approximation (TDA)[19] was used, as we found full TDDFT results unreliable. To validate the TDDFT optimization of T_1, structures optimized with unrestricted ground-state DFT BP/SV(P) and a spin multiplicity of 3 were also examined as they are supposed to give a good description of the lowest-energy electronic triplet states. Additional calculations of ground and excited state energies as well as transition moments were carried out at the spin-orbit complete active space self-consistent field (CASSCF) / complete active space second-order perturbation (CASPT2) level were performed for **1a** and **3c** at DFT-optimized S_0 and T_1 structures with default ANO basis sets contracted to Pt=7s6p4d2f1g, (C, N, O) = 3s2p1d, and H =2s1p using Molcas version 7.8.[20]An active space with

the LUMO and 17 occupied orbitals was used for **3c** in order to include most of the orbitals with significant Pt*5d* contributions. ACAS(2,2) level was employed for **1a**.

Additional calculated data

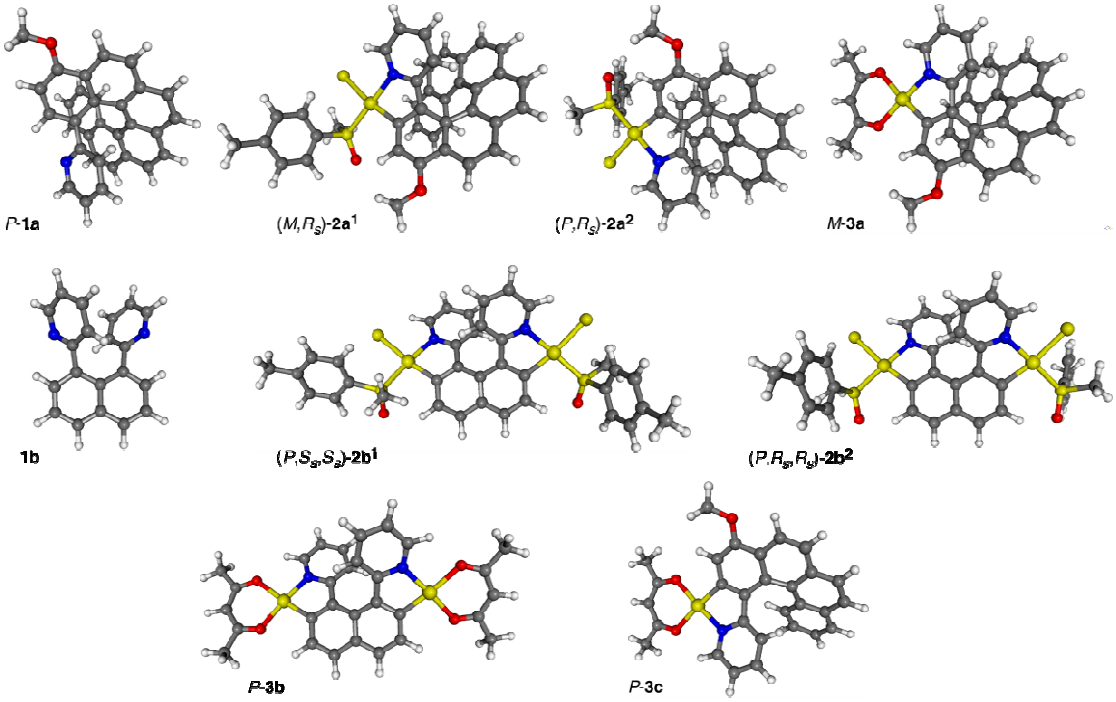

Figure S28. Structures and absolute configurations of mono- and bis-cycloplatinated helicene complexes and of the individual starting ligands.

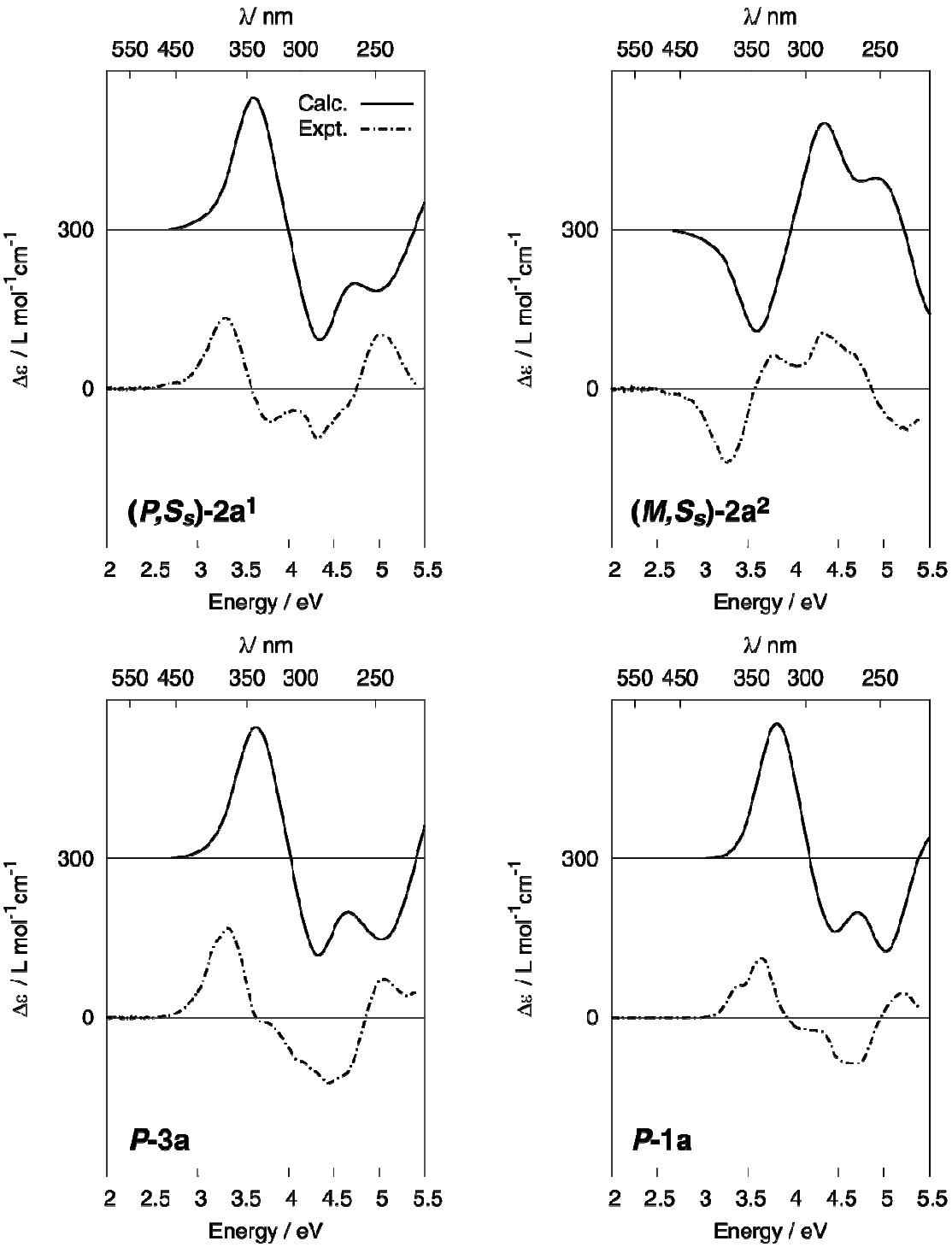

Figure S29. Comparison of experimental and TDDFT BHLYP/SV(P) calculated CD spectra of the '**a**' series of systems. No spectral shifts were applied.

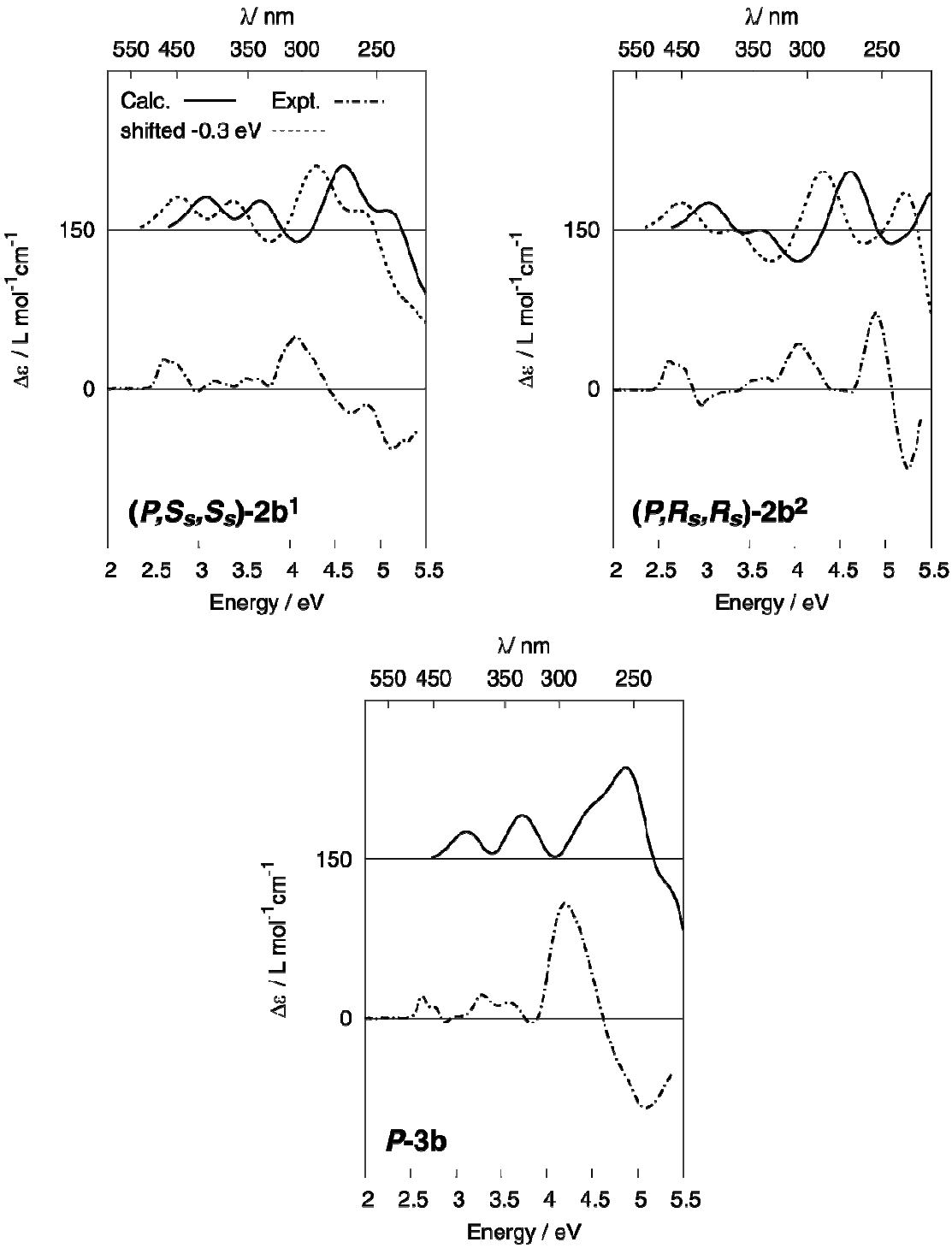

Figure S30. Comparison of experimental and TDDFT BHLYP/SV(P) calculated CD spectra of the '**b**' series of systems. No spectral shifts were applied except for **2b**^{1} as indicated.

Table S1. Optical rotations for the bis-cycloplatinatedhelicenes **2b**[2] and **3b** calculated with different basis sets and density functionals, and with different ways to eliminate gauge-origin dependence (MVG vs. GIAO).[a)]

	(P,R_S,R_S)-**2b**[2]		P-**3b**	
	$[\alpha]_D$	$[\phi]_D$	$[\alpha]_D$	$[\phi]_D$
Turbomole				
BHLYP/SV(P)	413.1	4337	1185	10297
NWChem				
BHLYP/SV(P)/MVG	497.3	5221	1198	10411
BHLYP/SV(P)/GIAO	---	---	1221	10606
CAM/SV(P)/MVG	486.0	5102	1189	10330
LC-PBE0/SV(P)/MVG	375.7	3944	997	8663
BHLYP/SVPD/MVG	515.4	5411	1242	10790
BHLYP/SVPD/GIAO	---	---	1066	9260
CAM/SVPD/MVG	494.4	5191	1240	10776
LC-PBE0/SVPD/MVG	380.8	3998	1035	8992
Expt. (23°C)		9616		8950

[a)] MVG: Modified Velocity Gauge, GIAO: Gauge-Including Atomic Orbitals, CAM: CAM-B3LYP. Specific and molar rotations in degree/(dm g/cm^{-3}) and degree cm^2/dmol, respectively.

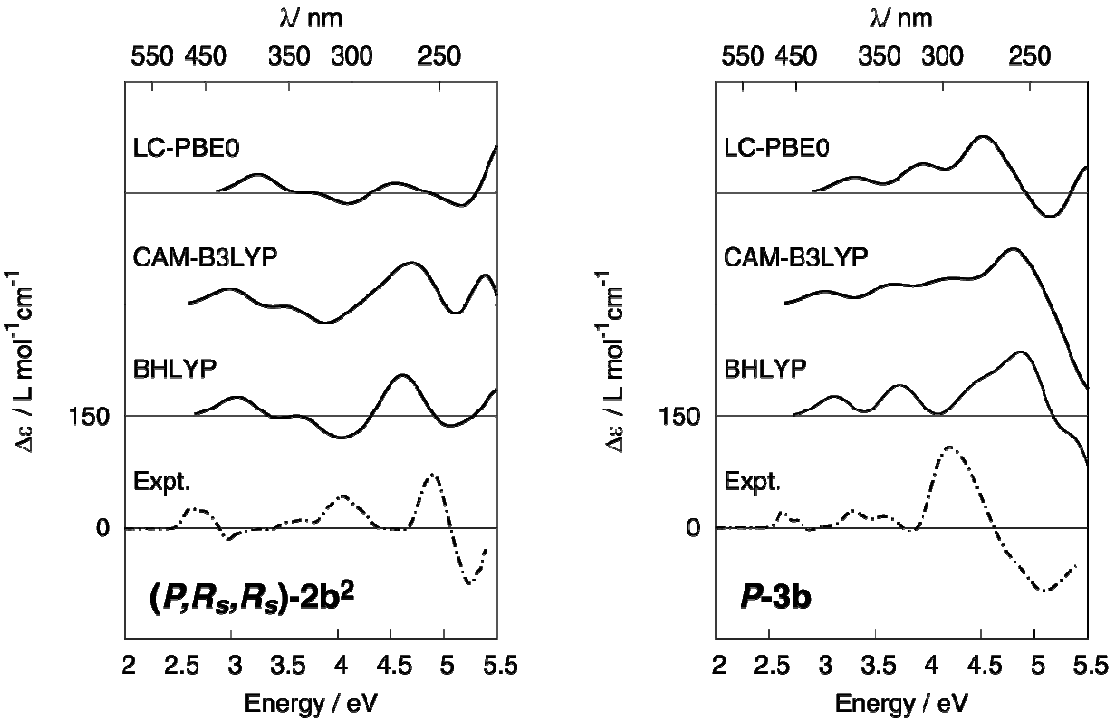

Figure S31. Comparison of experimental CD spectra for selected systems with calculations using different functionals. No spectral shifts were applied. SV(P) basis.

Table S2. Experimental and calculated optical rotations for the **2b**^{1,2} complexes and their **2b**^{1,2,} conformers, and relative energies of the conformers.[a)]

	ΔE^a / kcal/mol	BHLYP/SV(P) $[\alpha]_D$	BHLYP/SV(P) $[\phi]_D$	Expt. (23°C) $[\phi]_D$
(P,S_S,S_S)-**2b**^{1}	0.00	933.4	9800	11720
(P,S_S,S_S)-**2b**^{1,}	5.26	498.6	5234	
(P,R_S,R_S)-**2b**^{2}	0.00	413.1	4337	9616
(P,R_S,R_S)-**2b**^{2,}	13.72	823.5	8645	

[a)] Relative energy with respect to **2b**^{1} and **2b**^{2}. Specific and molar rotations in units of degree/(dm g cm^{-3}) and degree cm^2/dmol, respectively.

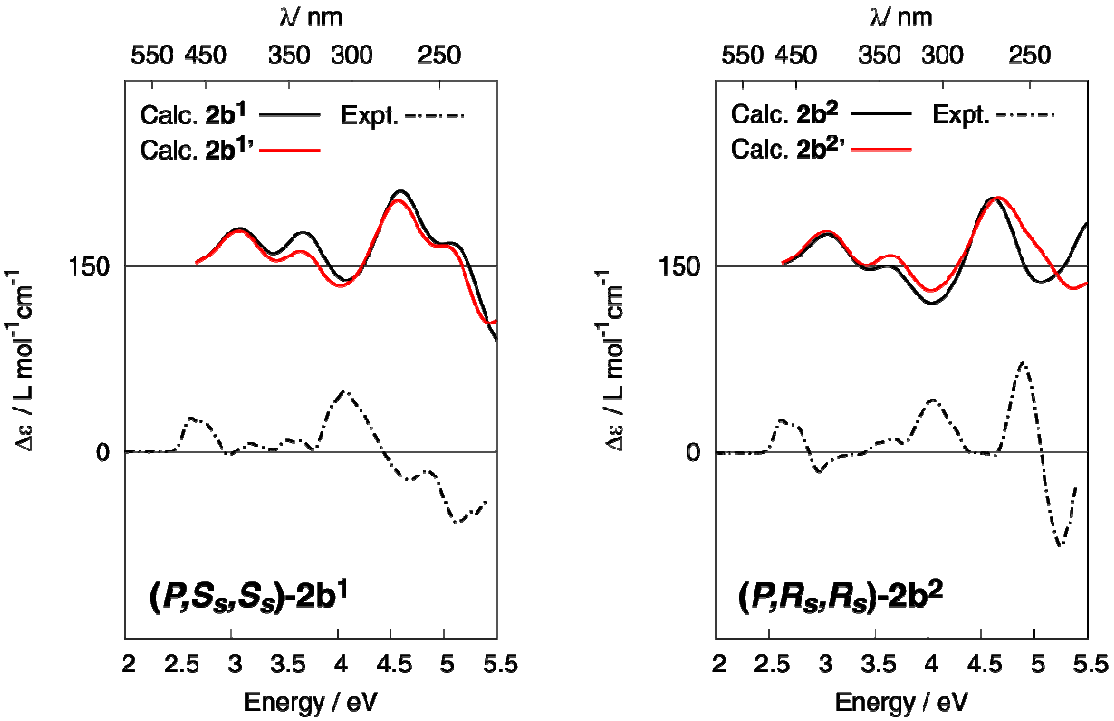

Figure S32. Comparison of the experimental and TDDFT BHLYP/SV(P) CD spectra calculated for the **2b**^{1} and **2b**^{2} conformers. No spectral shifts were applied.

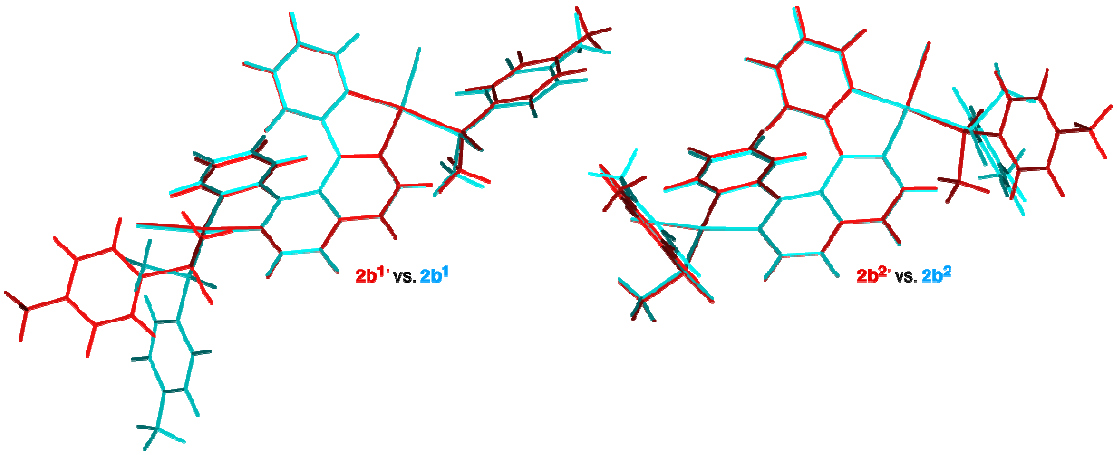

Figure S33. Overlays of optimized structures of **2b**^{1} and **2b**$^{1'}$, and **2b**^{2} and **2b**$^{2'}$.

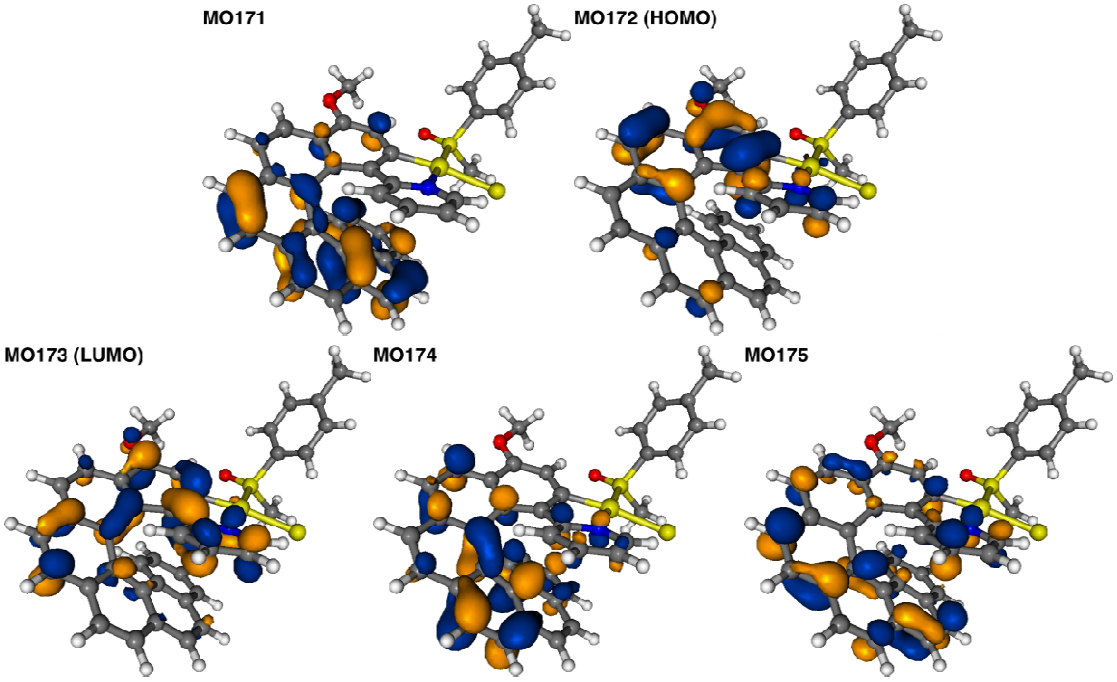

Figure S34. Isosurfaces (0.04 au) of MOs involved in selected excitations of **2a**^{1}.

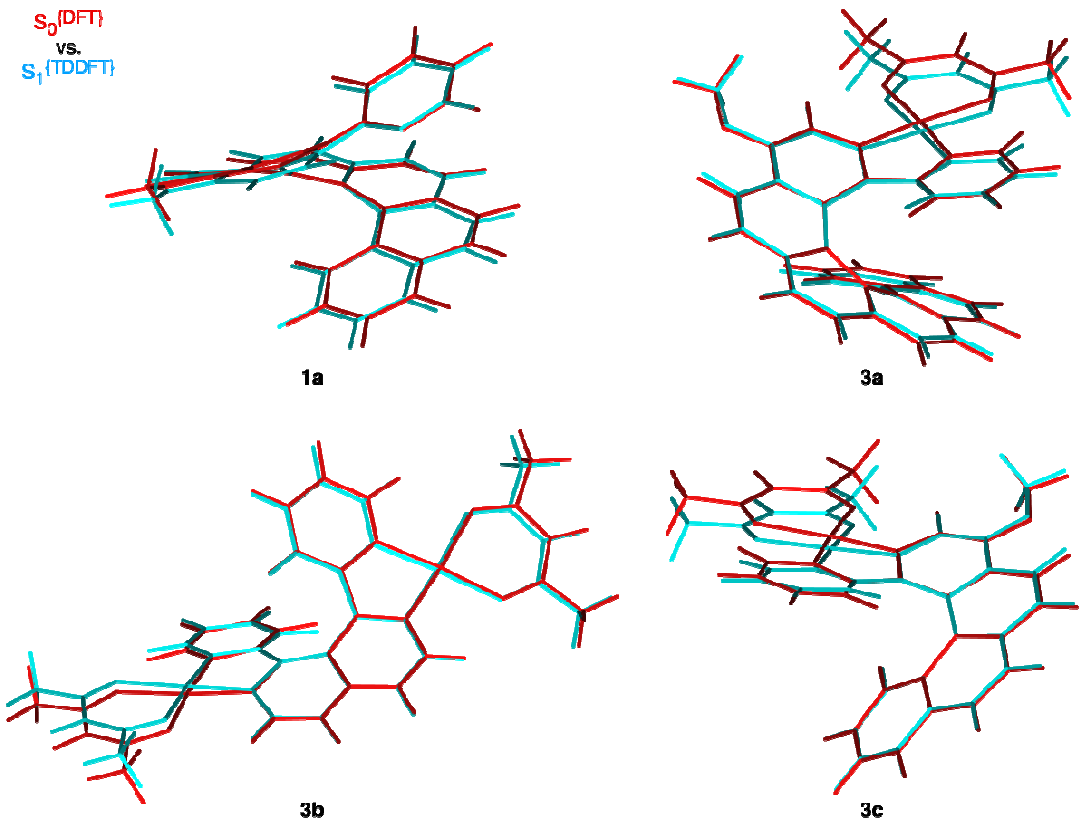

Figure S35. Overlays of optimized ground-state ($S_0^{\{DFT\}}$, red) and singlet excited-state ($S_1^{\{TDDFT\}}$, blue) structures of **1a** and **3a,b,c**.

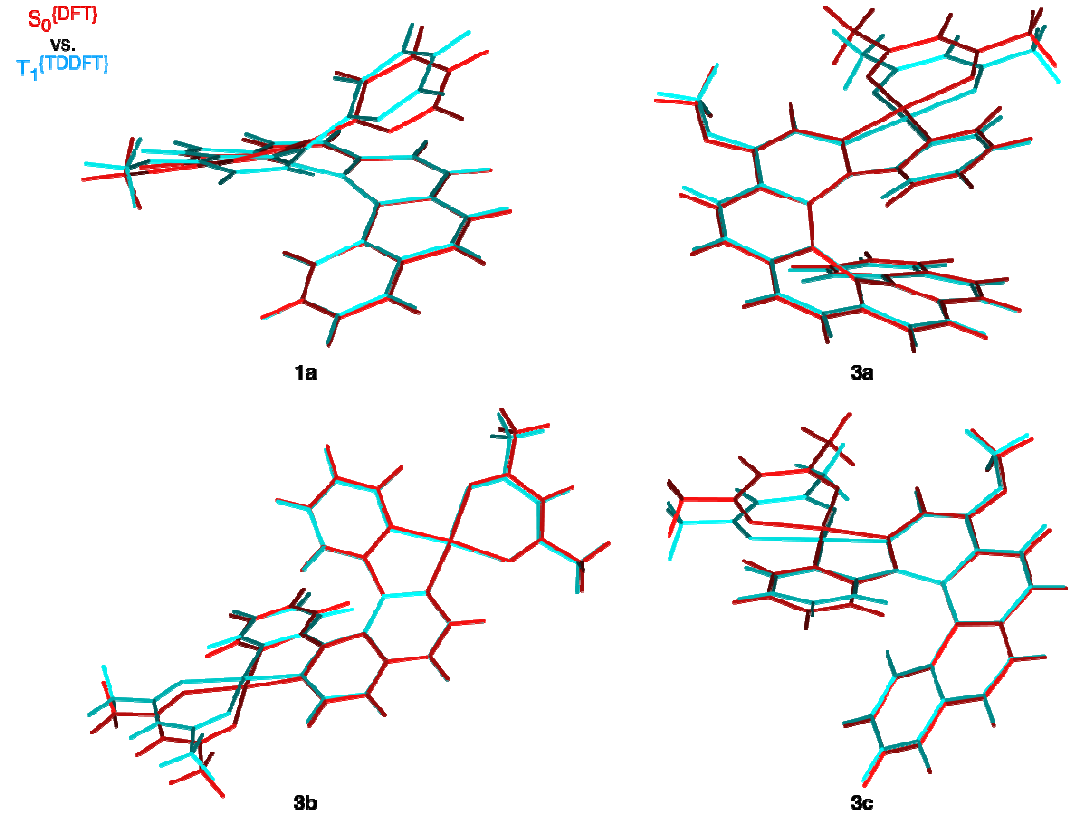

Figure S36. Overlays of optimized ground-state ($S_0^{\{DFT\}}$, red) and triplet excited-state ($T_1^{\{TDDFT\}}$, blue) structures of **1a** and **3a,b,c**.

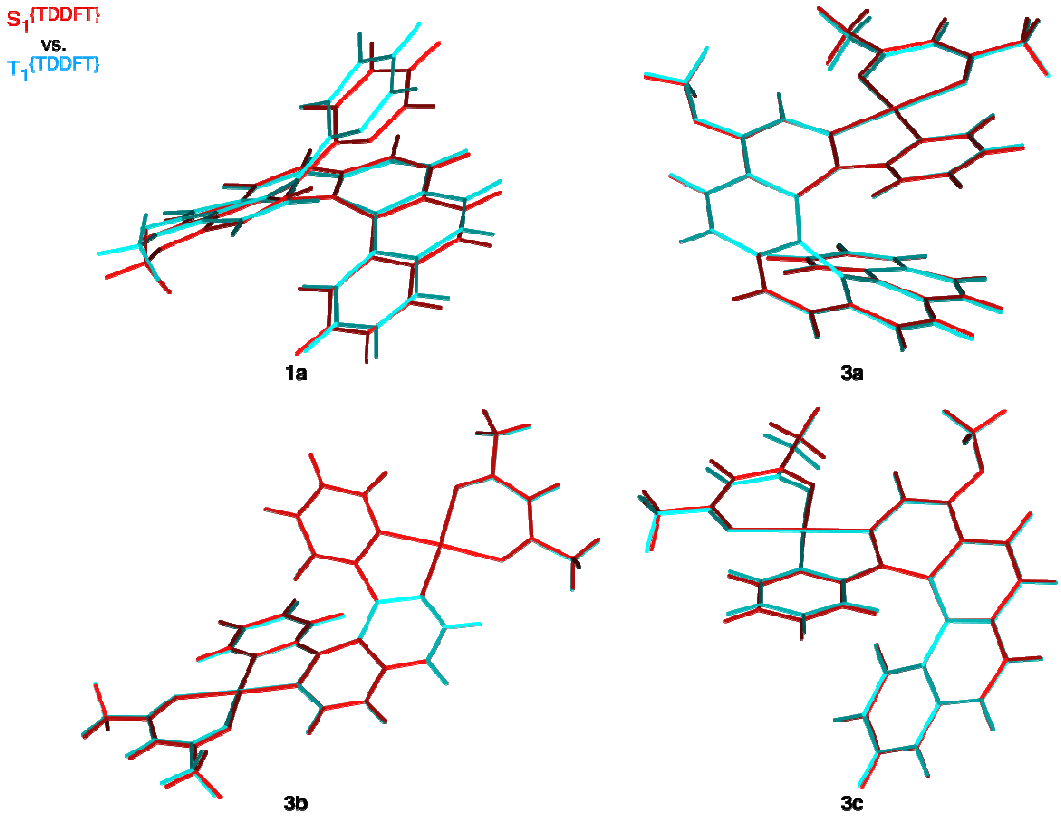

Figure S37. Overlays of optimized singlet excited-state ($S_1^{\{TDDFT\}}$, red) and triplet excited-state ($T_1^{\{TDDFT\}}$, blue) structures of **1a** and **3a,b,c**.

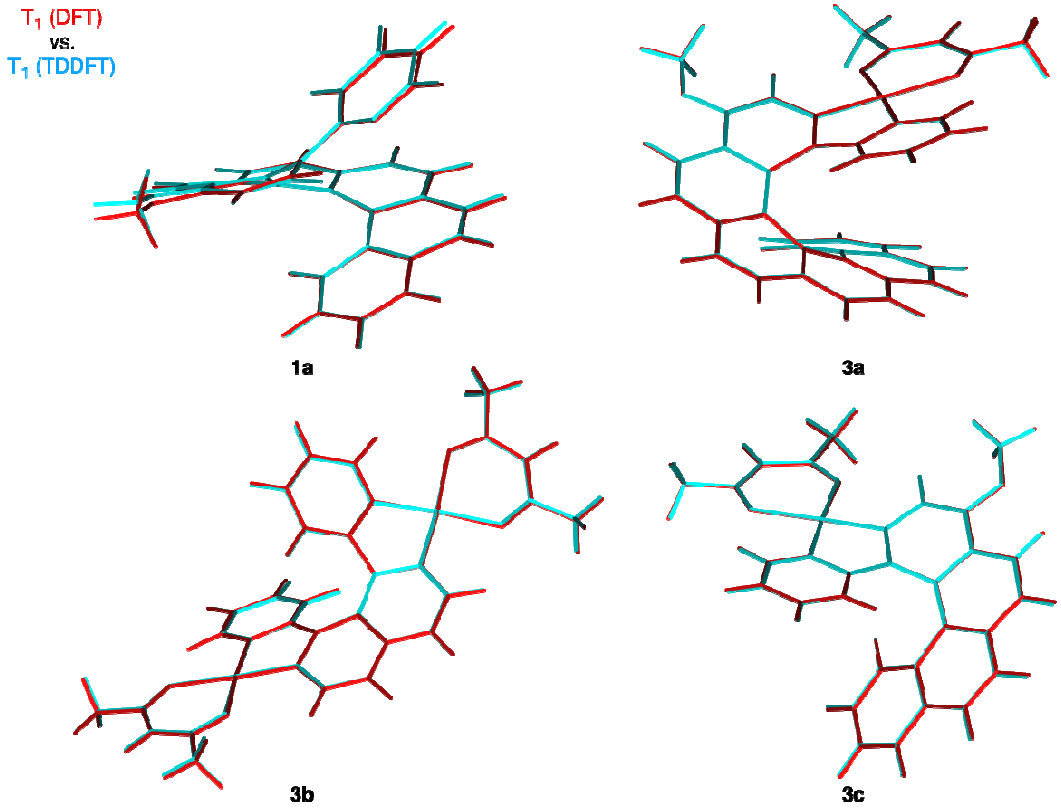

Figure S38. Overlays of optimized triplet excited-state ($T_1^{\{DFT\}}$, red) and triplet excited-state ($T_1^{\{TDDFT\}}$, blue) structures of **1a** and **3a,b,c**.

Table S3. Calculated BHLYP/SV(P) energy values, in au, of ground and excited states for ligand **1a** and mono- and bis-cycloplatinatedhelicenes**3a**,**b**,**c**. [a]

System	**1a**	**3a**	**3b**	**3c**
$S_0//S_0^{\{DFT\}}$	-1360.175152	-1823.566400	-1805.625278	-1516.717320
$T_1//T_1^{\{DFT\}}$	-1360.089661	-1823.487922	-1805.544491	-1516.638257
$S_0//T_1^{\{DFT\}}$	-1360.152239	-1823.554412	-1805.615490	-1516.704383
$T_1//S_0^{\{DFT\}}$	-1360.075143	-1823.479602	-1805.539381	-1516.629719
$S_0//S_1^{\{TDDFT\}}$	-1360.173640	-1823.578130	-1805.637346	-1516.724815
$S_0//T_1^{\{TDDFT\}}$	-1360.163152	-1823.574839	-1805.634673	-1516.721081

[a] spin state // geometry$^{\{method\}}$

Table S4. Calculated photophysical data, in eV, of ligand **1a** and of the mono-cycloplatinated helicene **3c**.[a]

System	**1a**	**3c**
	TDDFT S_0-S_1//S_0 {DFT}[b]	
E	3.47	3.25
f / *R*	0.0100 / 15.16	0.1377 / 22.67
Assignment	MO114-to-MO116: 31.7%	MO123-to-MO124: 89.4%
	MO114-to-MO115: 25.3%	
	MO113-to-MO116: 17.3%	
	MO113-to-MO115: 11.3%	
	CASSCF (CASPT2) S_0-S_1//S_0 {DFT}[c]	
E	4.64 (3.50)	4.23 (2.95)
f / *R*	0.5163 (0.3865) /	0.5438 (0.2794) /
	190.15 (189.70)	40.45 (41.92)
	TDDFTS_0-S_1//S_1 {TDDFT}[d]	
E	2.93	2.92
f / *R*	0.0477 / 390.92	0.1524 / 6.75
Assignment	MO114-to-MO115: 93.7%	MO123-to-MO124: 93.0%
	TDDFTS_0-T_1//T_1 {TDDFT}[e]	
E	1.63	1.89
Assignment	MO114-to-MO115: 80.3%	MO123-to-MO124: 88.9%
	TDDFTS_0-T_1//T_1 {DFT}[f]	
E	1.76	1.89
Assignment	MO114-to-MO115: 75.1%	MO123-to-MO124: 87.3%
	CASSCF (CASPT2) S_0-T_1//T_1 {DFT}[g]	
E	1.68 (2.42)	2.11 (2.05)
f / *R*	0.0000 (0.0000) /	$1.31\cdot10^{-6}$ ($1.35\cdot10^{-5}$) /
	0.0000 (0.0000)	$9.19\cdot10^{-5}$ ($1.57\cdot10^{-3}$)

[a] Energy*E* in eV, oscillator strength *f* in au, rotatory strength, *R* in 10^{-40}cgs.

[b] TDDFT S_0-S_1 transition at DFT BP/SV(P) optimized singlet configuration S_0.

[c] Spin-orbit CASSCF(CASPT2) S_0-S_1 transition at DFT BP/SV(P) optimized singlet configuration S_0.

[d] TDDFT S_0-S_1 transition at TDDFT BHLYP/SV(P) optimized S_1 geometry.

[e] TDDFT S_0-T_1transitionat TDDFT BHLYP/SV(P) optimized T_1 geometry.

[f] TDDFT S_0-T_1 transition at DFT BP/SV(P) optimized triplet configuration.

[g] Spin-orbit CASSCF(CASPT2) S_0-T_1 transition at DFT BP/SV(P) optimized triplet configuration.

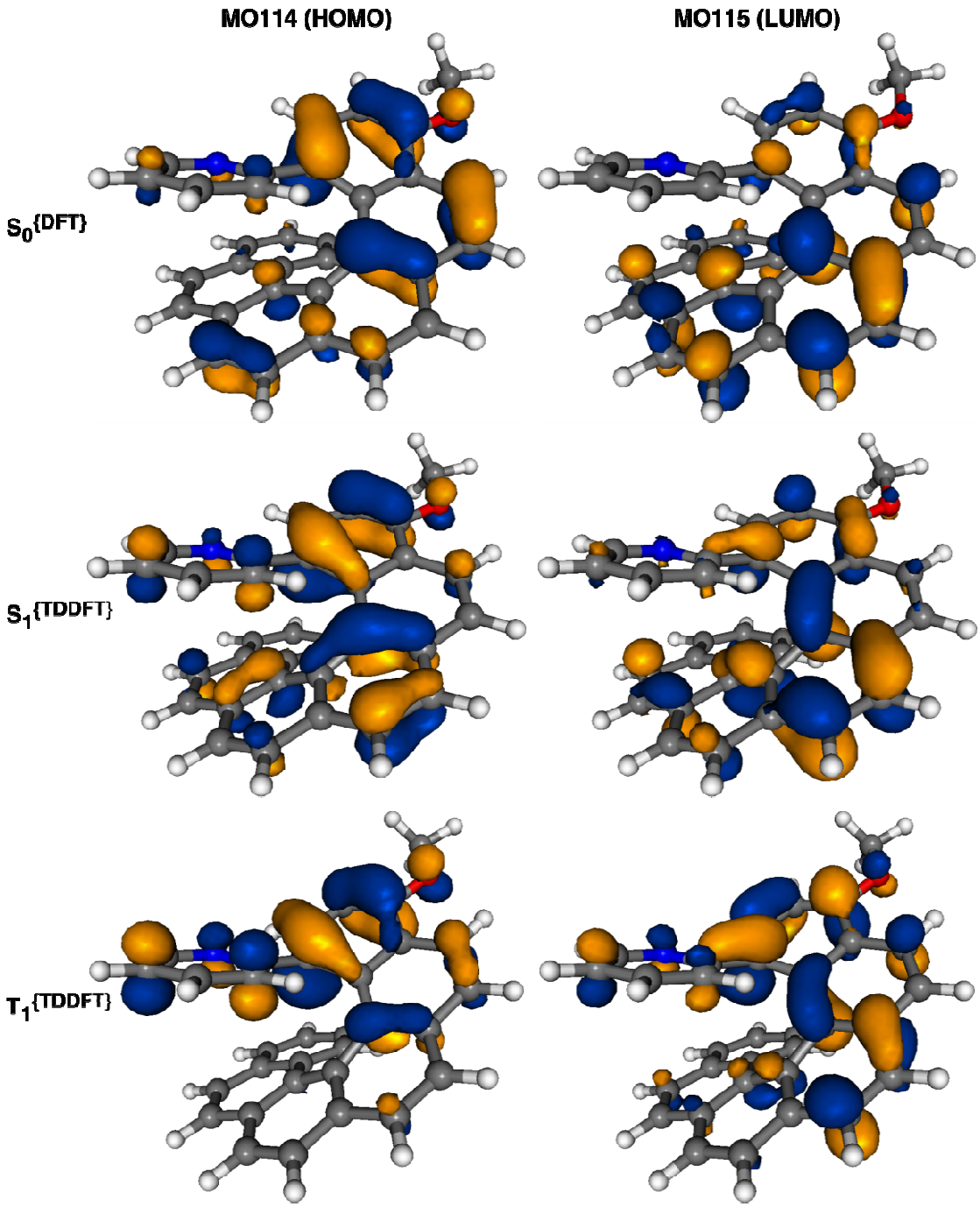

Figure S39. Isosurfaces (0.04 au) of frontier MOs in **1a** for $S_0^{\{DFT\}}$, $S_1^{\{TDDFT\}}$, and $T_1^{\{TDDFT\}}$ geometry.

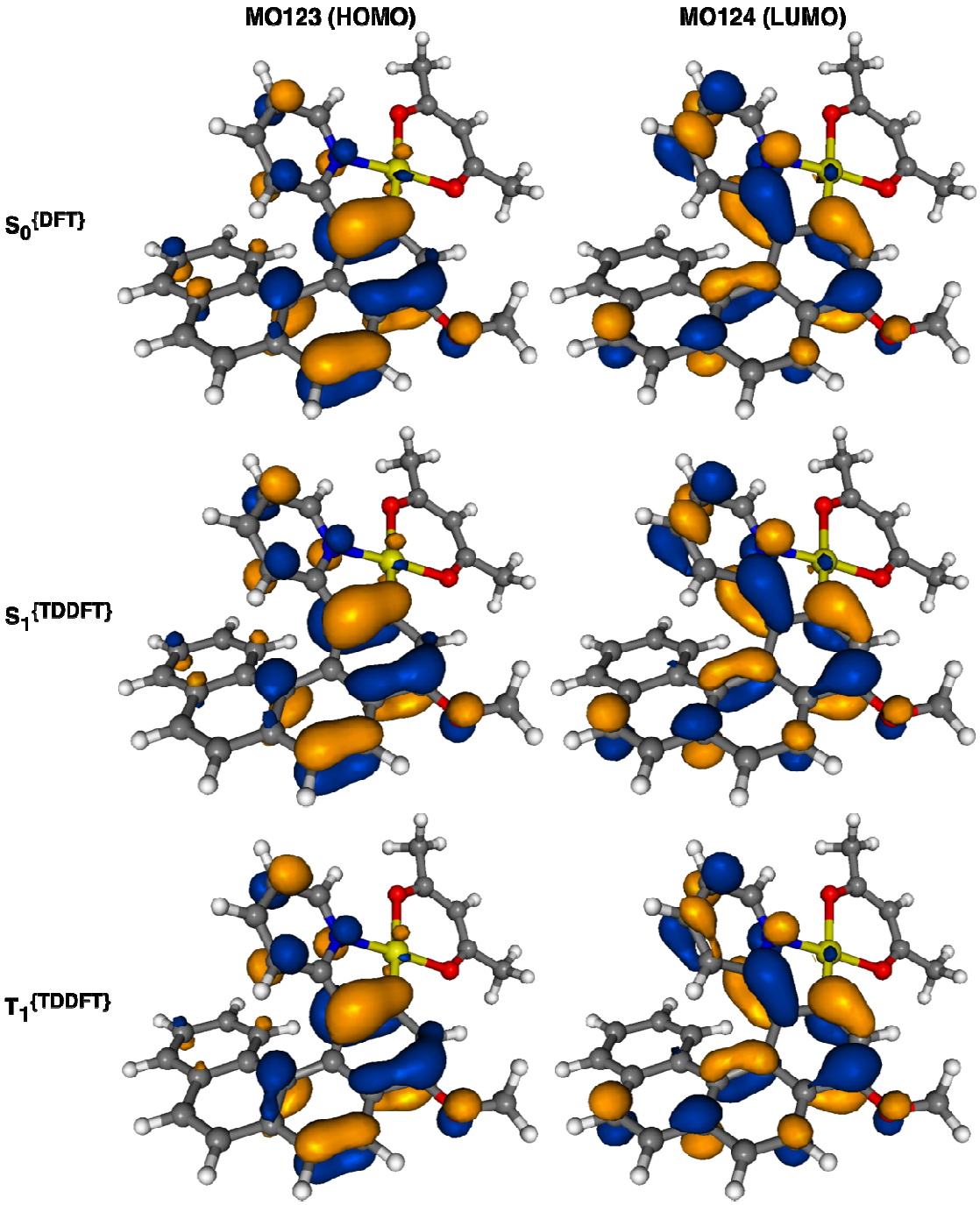

Figure S40. Isosurfaces (0.04 au) of frontier MOs in **3c** for $S_0^{\{DFT\}}$, $S_1^{\{TDDFT\}}$, and $T_1^{\{TDDFT\}}$ geometry.

[1] C. Shen, E. Anger, M. Srebro, N. Vanthuyne, L. Toupet, C. Roussel, J. Autschbach, R. Réau, J. Crassous, *Chem. Eur. J.,* 2013, **19**, 16728.
[2] (a) C. Wolf, X. Mei, *J. Am. Chem. Soc*., 2003, **125**, 10651. (b) X. Mei, R. M. Martin, C. Wolf, *J. Org. Chem.,* 2006, **71**, 2854.
[3] R. Romeo, L. Monsu Scolaro, *Inorganic Syntheses*, 1998, **32**, 153.
[4] S. R. Meech and D. Phillips, *J. Photochem.,* 1983, **23**, 193.
[5] J. Van Houten, and R. J. Watts, *J. Am. Chem. Soc.,* 1976, **98**, 4853.
[6] S. L. Murov, I. Carmichael, I. and G. L. Hug, *Handbook of Photochemistry,* 2nd ed., Marcel Dekker: New York, 1993.
[7] E. Brunet, L. Jiménez, M. de Victoria-Rodriguez, V. Luu, G. Muller, O. Juanes, J.C. Rodríguez-Ubis, *Microporous and Mesoporous Mater.*, 2013, **169**, 222 and references therein.
[8] H. P. J. M. Dekkers, P. F. Moraal, J. M. Timper, J. P. Riehl, *Appl. Spectrosc.,* 1985, **39**, 818.
[9] (a) *TURBOMOLE V5.7.1 2005, Quantum Chemistry Group, University of Karlsruhe, Germany*. (b) R. Ahlrichs, M. Bär, M. Häser, H. Horn, C. Kölmel, *Chem*. *Phys*. *Lett*. 1989, **162**, 165.
[10] (a) A. D. Becke, *Phys*. *Rev*. *A* 1988, **38**, 3098. (b) J. P. Perdew, *Phys*. *Rev*. *B* 1986, **33**, 8822. (c) J. P. Perdew, *Phys*. *Rev. B* 1986, **34**, 7406.
[11] (a) A. Schäfer, H. Horn, R. Ahlrichs, *J. Chem*. *Phys*. 1992, **97**, 2571. (b) K. Eichkorn, F. Weigend, O. Treutler, R. Ahlrichs, *Theor*. *Chem*. *Acc*. 1997, **97**, 119. (c) F. Weigend, R. Ahlrichs, *Phys*. *Chem*. *Chem*. *Phys*. 2005, **7**, 3297.
[12] D. Andrae, U. Häußermann, M. Dolg, H. Stroll, H. Preuß, *Theoret*. *Chim*. *Acta* 1990, **77**, 123.
[13] (a) C. Lee, W. Yang, R. G. Parr, *Phys*. *Rev*. *B* 1988, **37**, 785. (b) A. D. Becke, *J. Chem*. *Phys*. 1993, **98**, 1372.
[14] T. Yanai, D. P. Tew, N. C. Handy, *Chem*. *Phys*. *Lett*. 2004, **393**, 51.
[15] M. Srebro, N. Govind, W. A. de Jong, J. Autschbach, *J. Phys*. *Chem*. *A*, 2011, **115**, 10930.
[16] D. Rappoport, F. Furche, *J. Chem*. *Phys*. 2010, **133**, 134105-11.
[17] (a) E. J. Bylaska, W. A. de Jong, N. Govind, K. Kowalski, T. P. Straatsma, M. Valiev, J. J. van Dam, D. Wang, E. Apra, T. L. Windus, J. Hammond, J. Autschbach, F. Aquino, P. Nichols, S. Hirata, M. T. Hackler, Y. Zhao, P.-D. Fan, R. J. Harrison, M. Dupuis, D. M. A. Smith, K. Glaesemann, J. Nieplocha, V. Tipparaju, M. Krishnan, A. Vazquez-Mayagoitia, L. Jensen, M. Swart, Q. Wu, T. Van Voorhis, A. A. Auer, M. Nooijen, L. D. Crosby, E. Brown, G. Cisneros, G. I. Fann, H. Fruchtl, J. Garza, K. Hirao, R. Kendall, J. A. Nichols, K. Tsemekhman, K. Wolinski, J. Anchell, D. Bernholdt, P. Borowski, T. Clark, D. Clerc, H. Dachsel, M. Deegan, K. Dyall, D. Elwood, E. Glendening, M. Gutowski, A. Hess, J. Jaffe, B. Johnson, J. Ju, R. Kobayashi, R. Kutteh, Z. Lin, R. Littlefield, X. Long, B. Meng, T. Nakajima, S. Niu, L. Pollack, M. Rosing, G. Sandrone, M. Stave, H. Taylor, G. Thomas, J. van Lenthe, A. Wong, Z. Zhang, NWChem, A Computational Chemistry Package for Parallel Computers, Version 6.0 (2011 developer's version); Pacific Northwest National Laboratory, Richland, Washington 99352-0999, USA.; 2011. (b) M. Valiev, E. Bylaska, N. Govind, K. Kowalski, T. Straatsma, H. V. Dam, D. Wang, J. Nieplocha, E. Apra, T. Windus, W. de Jong, *Comput*. *Phys*. *Commun*. 2010, **181**, 1477. (c) J. Autschbach, *ChemPhysChem* 2011, **12**, 3224. (d) S. Hirata, C.-G. Zhan, E. Aprà, T.L. Windus, D.A. Dixon, *J. Phys*. *Chem*. *A,* 2003, **107**, 10154.
[18] J. Autschbach, T. Ziegler, S. J. A. van Gisbergen, E. J. Baerends, *J. Chem*. *Phys*. 2002, **116**, 6930.
[19](a) I. Tamm, *J. Phys*. (USSR) 1945, **9**, 449. (b) S. M. Dancoff, *Phys*. *Rev*. 1950, **78**, 382. (c) S. Hirata, M. Head-Gordon, *Chem*. *Phys*. *Lett*. 1999, **314**, 291. (d) M. J.G. Peach, M. J. Williamson, D.

J. Tozer, *J. Chem*. *Theory Comput*. 2011, **7**, 3578. (e) M. J. G. Peach, D. J. Tozer, *J. Chem*. *Phys*. *A* 2012, **116**, 9783. (f) M. J. G. Peach, N. Warner, D. J. Tozer, *Mol*. *Phys*. 2013, **111**, 1271.

[20] F. Aquilante, L. De Vico, N. Ferré, G. Ghigo, P.-å. Malmqvist, P. Neogrády, T. B. Pedersen, M. Pitoňák, M. Reiher, B. O. Roos, L. Serrano-Andrés, M. Urban, V. Veryazov, R. Lindh, *J. Comput*. *Chem*. 2010, **31**, 224.